

Structural basis for targeting the folded P-loop conformation of c-MET

Gavin W. Collie, Iacovos N. Michaelides, Kevin Embrey, Christopher J. Stubbs, Ulf Börjesson, Ian L. Dale, Arjan Snijder, Louise Barlind, Kun Song, Puneet Khurana, Christopher Phillips, and R. Ian Storer

Supporting information

Contents:

Supporting figures

Supporting tables

Materials and methods

Supporting information references and notes

Supporting figures

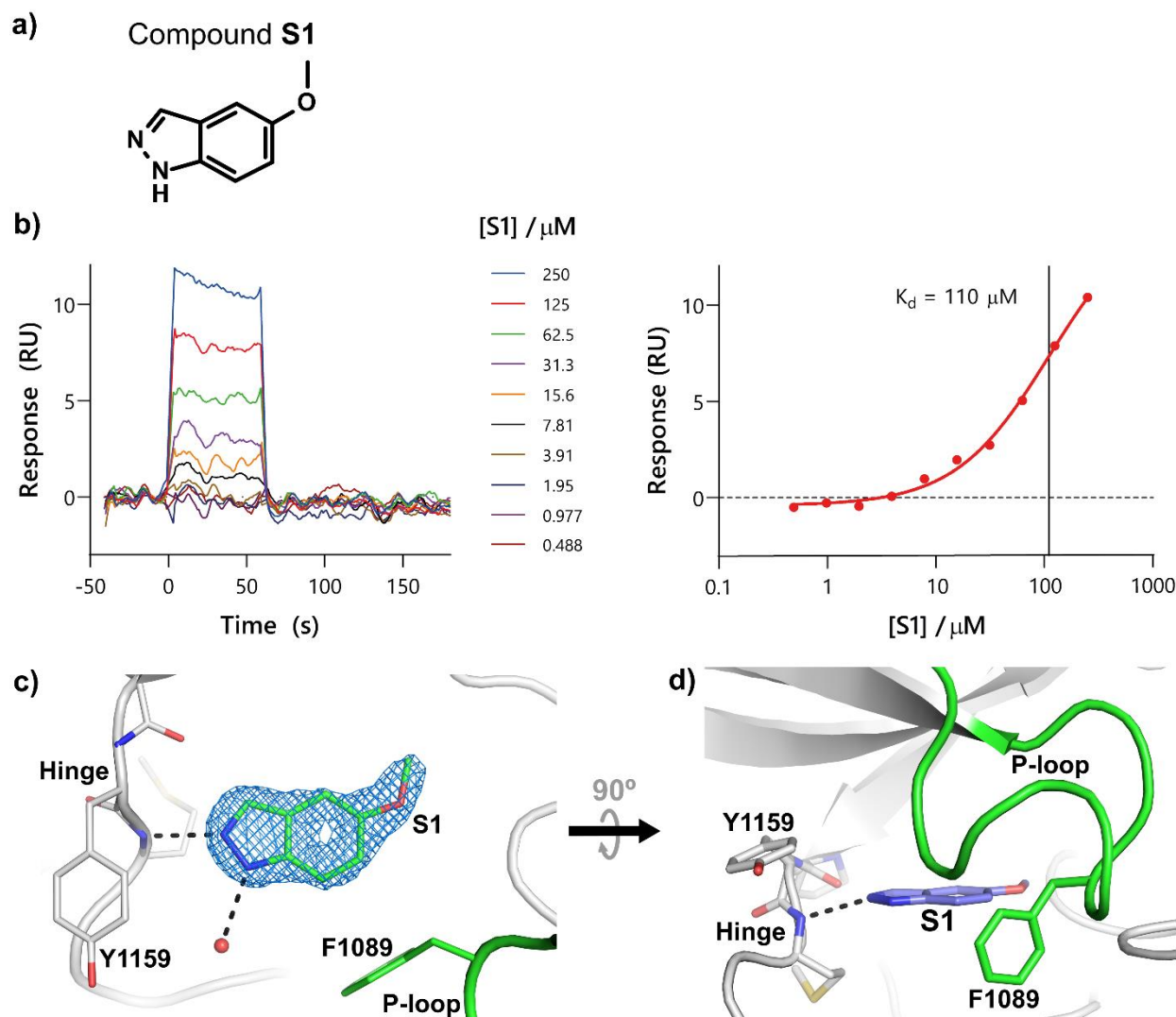


Figure S1. Identification of compound **S1** as a c-MET binder: biophysical and structural characterisation.

Compound **S1** (a) was identified as a primary hit for c-MET from the 1D NMR-based fragment screen described below and in the main manuscript. SPR analysis of this compound provided a K_d of 110 μM ($\pm 15 \mu\text{M}$) for c-MET (b). In order to assess the feasibility and suitability of using a soakable crystallographic system to characterise this and other hits from our screening efforts, crystals of c-MET in complex with compound **1** were soaked overnight in a 0.5 μL drop composed of the crystallisation reagent (detailed in Table S1) supplemented with a 10 mM concentration of compound **S1**. A 1.76 \AA crystal structure was determined for one of these soaked crystals, revealing clearly compound **S1** to: 1) have fully displaced compound **1** (c), and 2) bind to the folded P-loop conformation of the protein (d). This method therefore potentially provided an easy and rapid means of structurally characterising the NMR-derived fragment hits for c-MET. However, while the electron density for compound **S1** bound to c-MET was unambiguous (c), this compound is known to bind to kinase hinge regions *via* both nitrogen atoms (data not shown). Such a binding mode is not compatible with the folded P-loop conformation due to a steric clash between the methoxy group of **S1** and residue F1089 of the P-loop, and we were therefore concerned that this soakable crystal system may generate binding modes not representative of the solution behaviour of the compounds studied. As a result, all further ligand-complex structures were determined by co-crystallisation using sparse matrix screens in order to ensure a broader sampling of conformational space. However, we note that the soakable system we describe here may facilitate the screening of fragments, for example by in-crystal fragment screening, as a means to find novel chemical scaffolds able to bind to the folded P-loop conformation of c-MET. The crystal structure of c-MET bound by compound **S1** has been deposited in the Protein Data Bank with accession code and further details provided in Table S1. Electron density map (blue mesh) shown in (c) is a $2F_o - F_c$ map shown at a σ level of 1.8.

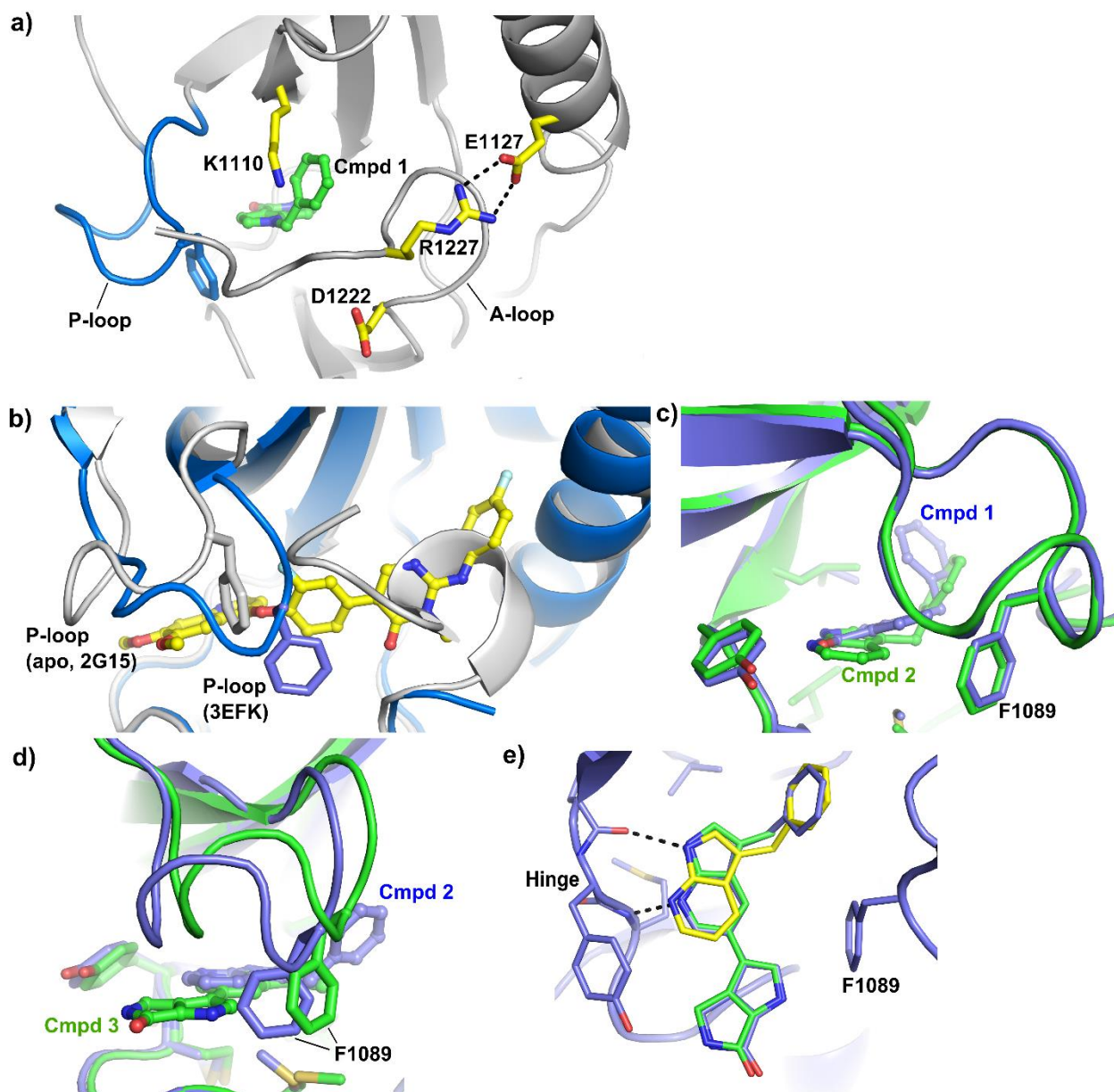


Figure S2. Supporting crystallographic figures.

a) Crystal structure of c-MET-compound 1 complex highlighting the separation of several key catalytic residues (yellow sticks) by the A-loop. The folded P-loop is highlighted blue. b) Overlay of the apo c-MET crystal structure (white, PDB entry 2G15¹) with the ligand complex reported by D'Angelo et al. (blue, PDB entry 3EFK²). c) Structural alignment of c-MET-compound 1 (blue) and c-MET-compound 2 (green) crystal structures. d) Structural alignment of c-MET-compound 2 (blue) and c-MET-compound 3 (green) crystal structures, highlighting difference in P-loop position. e) Alignment of compounds 2 (yellow), 3 (green) and 5 (blue) from c-MET complexes.

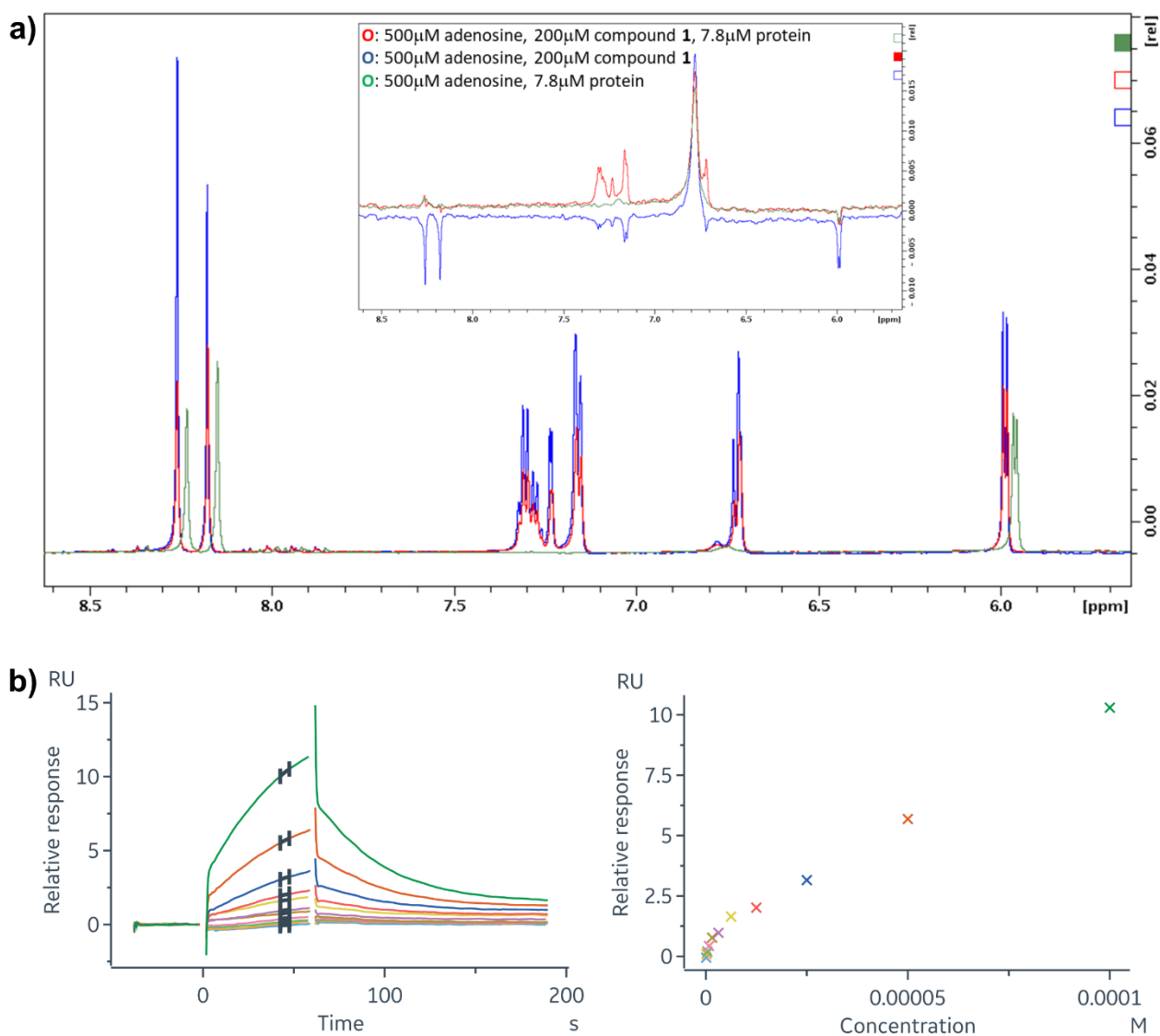
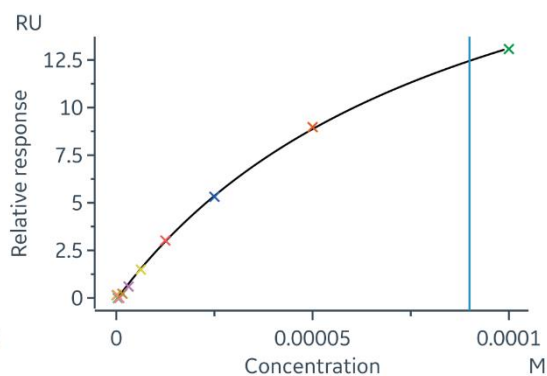
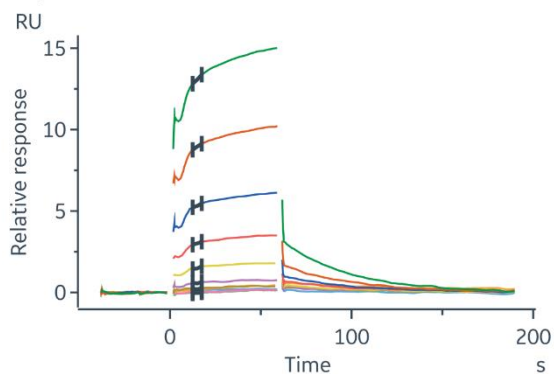


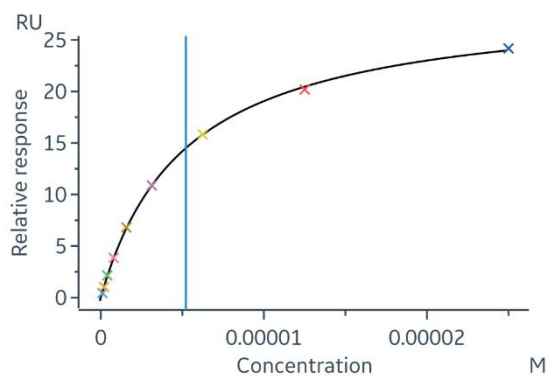
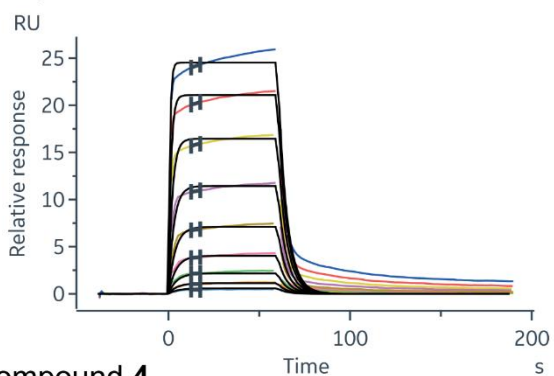
Figure S3. Identification of compound 1 – NMR and SPR data.

a) CPMG spectrum of compound **1** in the presence and absence of recombinant c-MET protein, with WaterLOGSY spectra shown in the insert. Adenosine was included in these experiments in order to provide an early indicator of the possible site of fragment binding. Protein refers to the kinase domain of wild-type c-MET (further details below). The lack of competition with adenosine, in combination with the crystallographic data, indicates compound **1** to be a weak hinge binder. b) Representative SPR sensorgram for compound **1** binding to immobilised c-MET. Further experimental details can be found below and in Collie et al., 2019.³

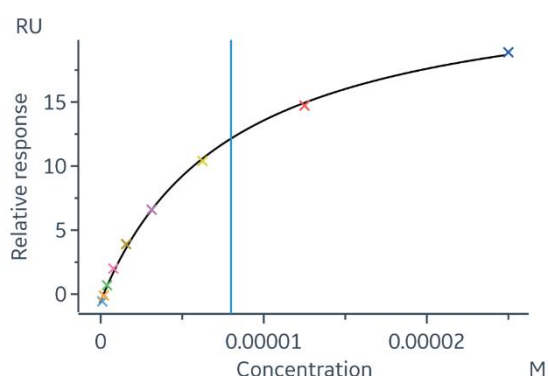
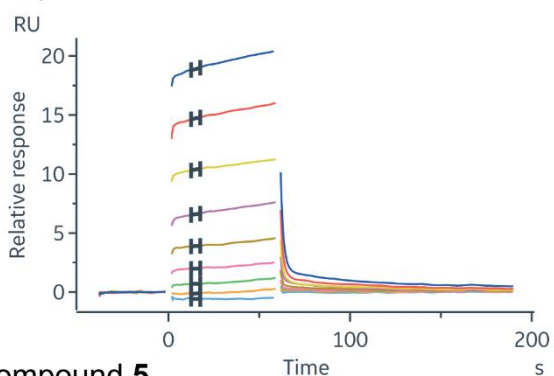
Compound 2



Compound 3



Compound 4



Compound 5

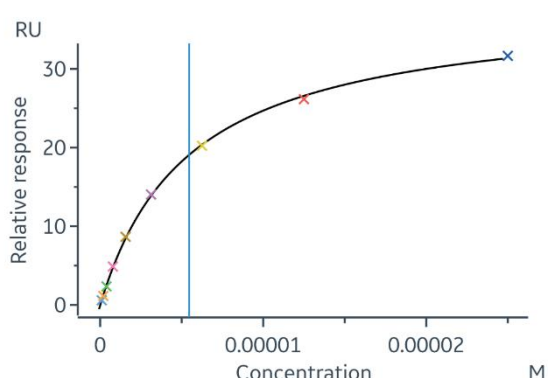
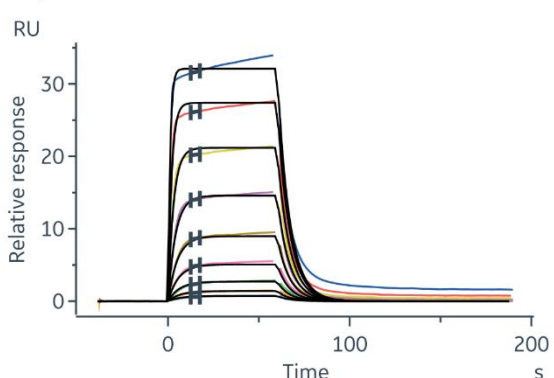


Figure S4. Representative SPR sensorgrams for compounds 2-5.

Compounds 2-5 were tested for binding to the intracellular domain of wild-type c-MET. Dissociation constants derived from these sensorgrams can be found in Table 1, and further experimental details can be found below and in Collie et al., 2019.³

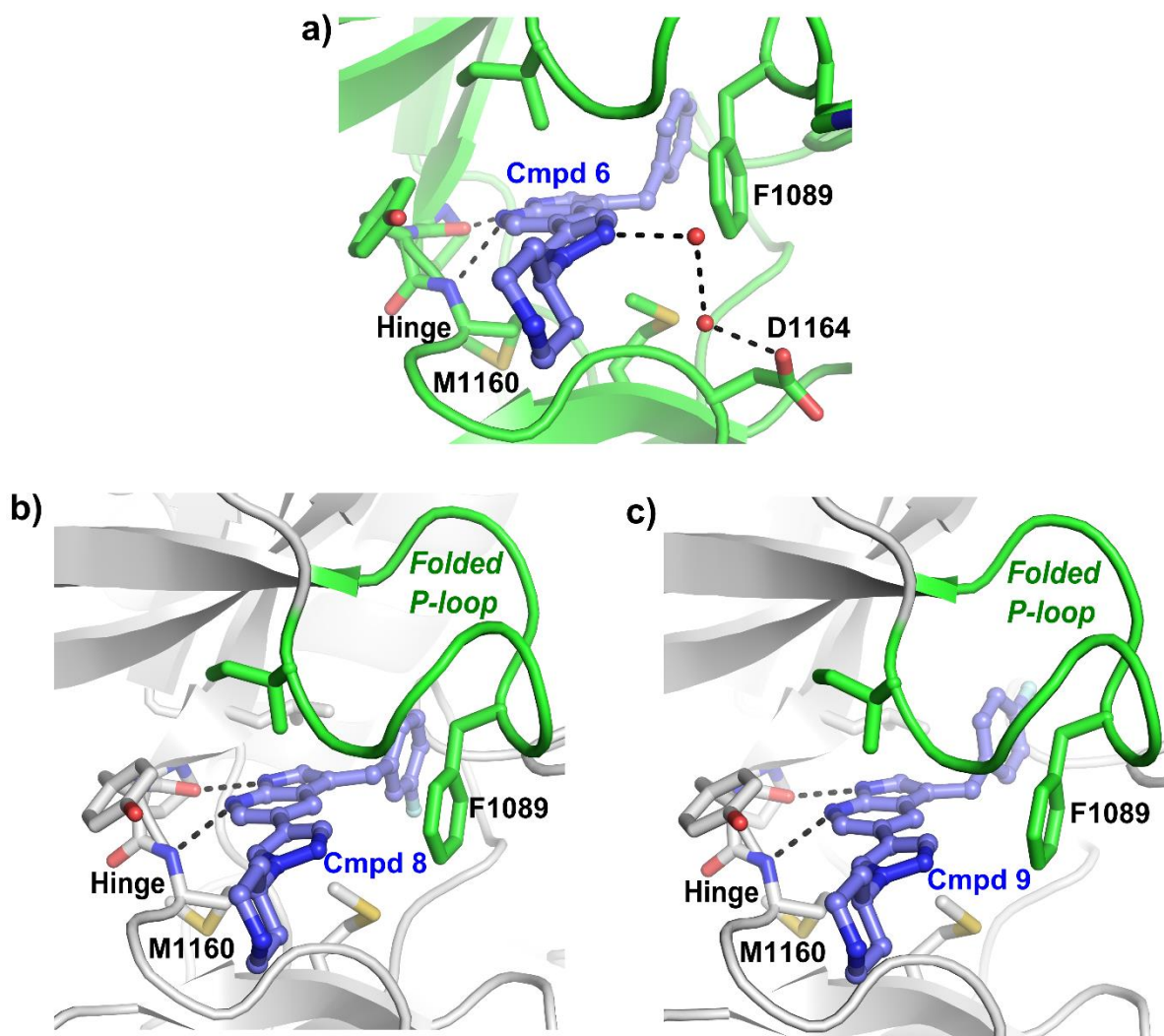


Figure S5. Supplementary figures of crystal structures of c-MET bound by compounds **6** (a), **8** (b) and **9** (c). Water molecules in (a) are shown as red spheres with hydrogen bonds shown as black dashes. Further details can be found in Table S1.

Supporting tables

Table S1. Details of crystallisation conditions and crystallographic data collection and refinement statistics for c-MET-small molecule crystal structures reported in this work (compounds **1-9** and **S1**)

Compound	1	2	3	4	5	
Crystallisation conditions	25 % PEG3350, 0.2 M (NH ₄) ₂ SO ₄ , 0.1 M Na-HEPES pH 7.5	25 % PEG8000, 0.2 M Li ₂ SO ₄	25 % PEG3350, 0.2 M (NH ₄) ₂ SO ₄ , PCPT ^a pH 5.5	8 % ethylene glycol, 10 % PEG8000, 0.1 M Na-HEPES pH 7.5	20 % PEG10000, 0.1 M Na-HEPES pH 7.5	
Cryo protection	No cryo	25 % PEG8000, 0.2 M Li ₂ SO ₄	No cryo	Above solution plus 25 % glycerol	Above solution plus 25 % glycerol	
Data Collection						
Space group	<i>C2</i>	<i>C2</i>	<i>C2</i>	<i>P4₁2₁2</i>	<i>C2</i>	
Unit cell	a, b, c (Å)	111.38, 42.59, 85.88	111.57, 43.04, 86.33	111.65, 42.79, 86.14	66.82, 66.82, 188.63	109.88, 42.45, 85.60
	α, β, γ (°)	90.00, 120.74, 90.00	90.00, 123.79, 90.00	90.00, 121.29, 90.00	90.00, 90.00, 90.00	90.00, 120.86, 90.00
Resolution (Å)	28.63 – 1.75 (1.85 – 1.75)	27.73 – 2.23 (2.27 – 2.23)	28.71 – 1.93 (1.96 – 1.93)	66.82 – 2.02 (2.05 – 2.02)	21.34 – 1.80 (1.83 – 1.80)	
R _{meas} (%)	2.5 (8.0)	6.1 (95.1)	5.0 (75.3)	8.2 (81.5)	7.1 (92.6)	
CC _{1/2} (%)	99.9 (99.2)	99.9 (49.3)	99.3 (93.6)	98.4 (60.3)	99.8 (54.8)	
I / σ	32.66 (9.82)	12.1 (1.3)	18.8 (2.6)	17.3 (2.8)	10.9 (1.2)	
Completeness (%)	95.9 (80.1)	96 (81.2)	98.0 (93.9)	100.0 (98.1)	98.7 (93.0)	
Reflections (total)	103180	50112	83656	354700	95113	
Reflections (unique)	34024	16221	26013	29100	31317	
Redundancy	3.0	3.1	3.2	12.2	3.0	
Refinement						
Resolution (Å)	23.69 – 1.75	27.73 – 2.23	22.61 – 1.93	54.53 – 2.02	21.34 – 1.80	
R / R _{free} (%)	17.1 / 19.2	21.1 / 26.1	22.5 / 24.8	23.2 / 26.1	19.3 / 21.5	
Overall B-factor (Å ²)	24.56	62.99	28.99	41.11	37.64	
R.m.s. deviations						
Bond lengths (Å)	0.010	0.010	0.010	0.010	0.010	
Bond angles (°)	0.96	1.01	1.01	1.01	0.94	
PDB code	7B3Q	7B3T	7B3V	7B3W	7B3Z	

Table S1 continued

Compound	6	7	8	9	S1	
Crystallisation conditions	20 % PEG4000, 10 % isopropanol, 0.1 M Na-HEPES pH 7.5	25 % PEG3350, 0.2 M MgCl ₂ , 0.1 M bis-tris pH 5.5	25 % PEG3350, 0.2 M MgCl ₂ , 0.1 M bis-tris pH 6.5	28 % PEGMME2000, 0.1 M bis-tris pH 6.5	Compound soaked into c-MET-1 co-crystals	
Cryo protection	Above solution plus 25 % ethylene glycol	No cryo	No cryo	No cryo	No cryo	
Data Collection						
Space group	<i>C2</i>	<i>C2</i>	<i>C2</i>	<i>P1</i>	<i>C2</i>	
Unit cell	a, b, c (Å)	109.93, 42.47, 86.08	111.67 42.62 86.44	112.22, 42.86, 86.96	42.87, 59.74, 77.60	110.12, 42.55, 85.79
	α, β, γ (°)	90.00, 120.94, 90.00	90.00, 122.07, 90.00	90.00, 122.23, 90.00	76.51, 73.88, 69.25	90.00, 121.30, 90.00
Resolution (Å)	47.15 – 1.76 (1.79 – 1.76)	47.32 – 1.97 (2.0 – 1.97)	55.63 – 1.80 (1.83 – 1.80)	73.71 – 1.87 (2.02 – 1.87)	38.77 – 1.76 (1.79 – 1.76)	
R _{meas} (%)	12.0 (154)	15.7 (185)	14.3 (213)	13.6 (64.2)	7.3 (105)	
CC _{1/2} (%)	99.5 (47.4)	99.4 (40.3)	99.6 (44.4)	98.5 (74.1)	99.8 (45.0)	
I / σ	7.9 (1.1)	7.7 (1.2)	9.3 (1.2)	3.8 (1.4)	10.8 (1.0)	
Completeness (%)	92.9 (99.3)	95.6 (96.3)	96.0 (99.5)	70.0 (34.6) ^b	97.0 (82.9)	
Reflections (total)	153996	119240	154284	77457	99230	
Reflections (unique)	31621	23793	31290	28964	32999	
Redundancy	4.9	5.0	4.9	2.7	3.0	
Refinement						
Resolution (Å)	47.15 – 1.76	47.31 – 1.97	55.62 – 1.80	18.41 – 1.87	23.01 – 1.76	
R / R _{free} (%)	19.6 / 23.2	19.6 / 23.3	20.2 / 22.5	20.0 / 24.8	17.8 / 20.8	
Overall B-factor (Å ²)	36.83	42.06	39.80	27.59	36.28	
R.m.s. deviations						
Bond lengths (Å)	0.010	0.010	0.010	0.010	0.010	
Bond angles (°)	0.97	1.02	0.99	1.02	0.99	
PDB code	7B40	7B41	7B42	7B43	7B44	

^a PCPT: Sodium propionate, sodium cacodylate trihydrate, bis-tris propane.

^b Dataset anisotropy corrected using STARANISO (Global Phasing Ltd.).

Table S2. Kinase selectivity data* for **7** at 100 nM

Kinase Name	Mean Inhibition (%)
NTRK3 (TRKC)	99
CSF1R (FMS)	98
JAK2	97
NTRK2 (TRKB)	96
LCK	96
NTRK1 (TRKA)	94
JAK3	94
MAP4K1 (HPK1)	92
AURKC (Aurora C)	92
NUAK1 (ARK5)	90
AURKB (Aurora B)	89
ABL1	88
TNIK	88
ROS1	88
TGFBR1 (ALK5)	86
MINK1	84
RET	83
ABL2 (Arg)	78
ALK	72
KDR (VEGFR2)	69
FLT3	68
EPHB1	66
MET (cMet)	66
MAP4K3 (GLK)	66
AXL	63
PEAK1	62
JAK1	60
FGFR2	57
YES1	57
DMPK	57
LYN A	57
PDGFRB (PDGFR beta)	56
MAP3K7/MAP3K7IP1 (TAK1-TAB1)	56
EPHA5	55
STK4 (MST1)	54
SRC	53
BLK	50
EPHB4	50
FYN	49
ULK2	48
MERTK (cMER)	46
STK17A (DRAK1)	45
RET V804L	44
MST1R (RON)	44
LRRK2	43
BTK	41
AAK1	40
FGFR1 V561M	39
DDR2	38
PTK2 (FAK)	37
RET V804M	37
CLK2	35
FER	33
CLK4	32
KIT	32
FGFR1	29
ACVR1B (ALK4)	28
IRAK1	25
CDK1/cyclin B	25
TYRO3 (RSE)	22
BMX	22
RPS6KB1 (p70S6K)	22
MARK2	20
FLT1 (VEGFR1)	19
AMPK A2/B1/G1	19
CDK7/cyclin H/MNAT1	19
MARK1 (MARK)	18
MAP3K9 (MLK1)	17
PRKACA (PKA)	17

PTK6 (Brk)	16
IRAK4	15
CLK1	15
IGF1R	15
GSG2 (Haspin)	15
CDK9/cyclin T1	14
FES (FPS)	14
INSR	14
PRKCQ (PKC theta)	14
SYK	14
TBK1	14
CHEK1 (CHK1)	13
ROCK1	13
CLK3	13
PAK1	13
CDK2/cyclin A	12
CDK2/cyclin E1	10
PIK3C3 (hVPS34)	10
GSK3B (GSK3 beta)	9
FGFR3	9
MAP2K1 (MEK1)	9
GSK3A (GSK3 alpha)	9
ROCK2	8
MAPK14 (p38 alpha) Direct	8
FGFR4	8
PAK2 (PAK65)	7
AKT1 (PKB alpha)	7
BRAF	7
EGFR (ErbB1) T790M L858R	6
MAPKAPK2	6
MAPK1 (ERK2)	6
INSRR (IRR)	6
PRKCA (PKC alpha)	5
PAK7 (KIAA1264)	5
PIM2	5
PAK4	4
DYRK2	4
MAPK8 (JNK1)	4
RPS6KA1 (RSK1)	4
NEK2	4
RAF1 (cRAF) Y340D Y341D	3
DNA-PK	3
MYLK (MLCK)	3
MAPKAPK5 (PRAK)	3
PI4KB (PI4K beta)	3
FRAP1 (mTOR)	3
PRKCE (PKC epsilon)	2
PDK1	2
ZAP70	2
PLK1	2
CSNK2A2 (CK2 alpha 2)	1
SRPK1	1
MKNK2 (MNK2)	1
CAMK2B (CaMKII beta)	1
EEF2K	-1
CDK8/cyclin C	-1
CSNK1G1 (CK1 gamma 1)	-1
EGFR (ErbB1)	-1
AKT2 (PKB beta)	-1
PRKG1	-2
SGK (SGK1)	-3
PIK3CD/PIK3R1 (p110 delta/p85 alpha)	-3
IKKBK (IKK beta)	-3
ERBB2 (HER2)	-5
PIK3C2A (PI3K-C2 alpha)	-5
RPS6KA5 (MSK1)	-6
ERBB4 (HER4)	-8
PIK3CA/PIK3R1 (p110 alpha/p85 alpha)	-8
CAMK1 (CaMK1)	-9
PIK3CB/PIK3R1 (p110 beta/p85 alpha)	-9
PIK3CG (p110 gamma)	-18

*ThermoFisher SelectScreen Kinase Profiling Service

Materials and methods

Protein expression and purification

A detailed description of the protein expression and purification methods used here has been published previously,³ and will be described here in brief only. For crystallographic studies, synthetic DNA coding for residues 1049-1346 of the kinase domain of human wild-type c-MET with an N-terminal HN-tag followed by a TEV protease cleavage site was cloned into a pACYC Duet vector together with DNA encoding for catYopH(164-468).⁴ Plasmids were transformed into *E. coli* cells and protein produced using 5 L Bioreactor fed-batch cultures with IPTG induction according to methods described in Soini et al., 2008.⁵ Purification methods followed those reported previously.³ Protein for NMR experiments was produced following a similar protocol, with the final purified protein encompassing residues 1038-1346. For biochemical assays and SPR analysis, a c-MET construct comprising residues 956-1390 with N-terminal HN-tag and avi-tags and a TEV protease recognition site were synthesised and cloned into pFastBac vectors. Protein expression was performed in Sf21 cells grown in wave-bioreactors or Thomson Optimum Growth flasks at 27 °C. Purification was performed as described previously.³ Where applicable, c-MET was biotinylated using BirA biotinylation kit (BirA-500, avidity) according to protocols described by the manufacturer. Samples were dephosphorylated using λ -phosphatase, where a 1:20 molar ratio of phosphatase to c-MET was applied. After confirmation of dephosphorylation by MS, c-MET was purified either by captoQ purification or by an additional size-exclusion purification.

NMR screening

A 1D NMR screening strategy was designed to identify fragment hits for the kinase domain of c-MET. Screening mixtures contained 6 fragments at 200 μ M and adenosine at 500 μ M in 25 mM HEPES pH 7.5, 50 mM NaCl, 2 mM MgCl₂, 0.02% NaN₃, 5% D₂O and Carr-Purcell-Meiboom-Gill sequence (CPMG) and WaterLOGSY⁶ NMR screening experiments were recorded in the presence and absence of 7.8 μ M wild-type c-MET comprising the kinase domain only (residues 1038-1346). Adenosine was included as a means to provide information concerning the potential binding site of resultant fragment hits. All NMR spectra were collected on a Bruker Avance III 600 MHz spectrometer with a triple resonance inverse cryoprobe equipped with z-axis gradient.

Surface plasmon resonance (SPR)

SPR experiments were performed on wild-type c-MET protein encompassing residues 956-1390, as described above. A description of the SPR methods used in this work has been reported previously³ with the slight differences that, in this current work, EDC/NHS was injected for 120 s and the protein injected for 300 s.

Crystallography

For crystallisation trials, dephosphorylated protein comprising the kinase domain of wild-type c-MET (encompassing residues 1049-1346) was used at a concentration of approximately 10 mg/ml. Prior to crystallisation, compounds **1-9** were added to protein samples to final concentrations of 1-2 mM from 100 mM stocks in 100 % DMSO, equivalent to a 3-6-fold molar excess of compound over protein. Co-crystals were grown at 20 °C in sitting drops composed of 100 nL of protein-inhibitor complex plus an equal volume of crystallisation reagent. Each protein-inhibitor complex was screened against a broad range of crystallisation conditions using a sparse-matrix approach. Details of crystallisation and cryo-protection conditions for each protein-inhibitor complex can be found in Table S1. Compound **S1** was soaked into crystals of c-MET bound by compound **1**, with further details provided in Figure S1. X-ray diffraction data were collected at the Swiss Light Source and Diamond Light Source synchrotrons. Data were processed using XDS,⁷ xia2,⁸ DIALS⁹, autoPROC¹⁰, STARANISO (Global Phasing Ltd.) (dataset for compound **9** only) and CCP4,¹¹ and structures solved by molecular replacement using publicly available c-MET structures^{1,12} using Phaser¹³ from the CCP4 package.¹¹ Model building and refinement were performed using Coot¹⁴ and Buster (Global Phasing Ltd.), respectively, with geometric restraints for small molecule inhibitors generated in Grade (Global Phasing Ltd.). Data collection and refinement statistics plus PDB accession codes can be found in Table S1.

Biochemical enzyme inhibition assay

The ADP-Glo™ Kinase Assay (Promega) was used to determine the half maximal inhibitory concentration (IC₅₀) of the small molecule compounds reported in this work for wild-type c-MET following procedures described in full in Collie et al., 2019.³ Details of the protein construct used for these experiments can be found above.

Kinase selectivity

Compound **7** was screened at a concentration of 100 nM against a panel of 140 kinases using ThermoFisher's SelectScreen Kinase Profiling Service, with further details provided in Table S2.

Cellular homogeneous time-resolved FRET (HTRF) assay

Details of the homogeneous time-resolved FRET (HTRF) assay used in this work have been published previously.³ Briefly, NCI-H1993 cells were plated into tissue culture treated white HiBase low volume 384 well plates (Greiner BioOne) at 800 cells/well. Cells were allowed to adhere overnight by incubation under standard tissue culture conditions before treatment with test compounds, with additions made using an Echo 555 acoustic dispenser (Labcyte). Following a 4 hour incubation under standard tissue culture conditions, medium was removed from wells using a BlueWasher centrifugal plate washer (Blue Cat Bio) and 5 µl of phospho-cMET (Tyr1234/1235) HTRF lysis/detection reagent added (CisBio, AstraZeneca custom assay) using a Multidrop Combi dispenser (Thermo Fisher Scientific). Plates were sealed and incubated overnight in the dark before detection of HTRF signal (excitation 337 nm, emission 620/665 nm) using a Pherastar FS multimode reader (BMG Labtech).

Chemistry

General chemistry experimental procedures

Reagents and solvents (all anhydrous HPLC-grade) were obtained from commercial suppliers and used without any further purification unless otherwise stated. All reagents were weighed and handled in air unless otherwise stated. Brine refers to a saturated solution of NaCl. Concentration under reduced pressure refers to the use of a rotary evaporator.

Spectroscopy

¹H and ¹³C NMR spectra were recorded using Bruker Avance III, Avance III HD or Avance III NEO spectrometers at a proton frequency of 300 MHz, or a Bruker Avance Neo spectrometer at a proton frequency of 500 MHz. All ¹H and ¹³C NMR are quoted in ppm for measurement against TMS or residual solvent peaks as internal standards. Unless otherwise stated all experiments were carried out using DMSO-d₆ as solvent. ¹H NMR chemical shifts (δ) are given in ppm \pm 0.01, and coupling constants (J) are given in Hz \pm 0.1 Hz. The ¹H NMR spectra are reported as follows: δ /ppm (multiplicity, coupling constant(s) J /Hz, number of protons). Multiplicity is abbreviated as follows: s = singlet, br s = broad singlet, d = doublet, br d = broad doublet, dd = doublet of doublets, t = triplet, dt = doublet of triplet, q = quartet, dq = doublet of quartet, quint = quintet, m = multiplet. ¹³C NMR chemical shifts (δ) are given in ppm \pm 0.1.

MS experiments were performed using a Waters Acquity system combined with a Waters Xevo Q-ToF Mass or a Shimadzu 2010EV UPLC system in ESI mode. LC was run in two setups: 1) BEH C18 column (1.7 µm, 2.1 x 50 mm) in combination with a gradient (2-95% B in 5 minutes) of aqueous 46 mM ammonium carbonate/ammonia buffer at pH 10 (A) and MeCN (B) at a flow rate of 1.0 mL/min or in combination with a gradient (5-95% B in 2 minutes) of water and TFA (0.05%) (A) and CH₃CN and TFA (0.05%) at a flow rate of 1.0 mL/min (B).

Compound naming

Compound names are those generated by ChemDraw 19.0.

Compound purity

All compounds detailed below were found to be > 96% pure as assessed by LCMS. All HPLC was performed on an Agilent 1200 system (Agilent, Santa Clara, CA) comprising 2 G1312B ultra-high-pressure binary pumps, a G1315C Diode Array detector, a G1316B Column Compartment, a G1379B Micro De-gasser, a G1367C Micro Well Plate Auto-sampler and a 35900E analog-to-digital converter. The eluent from the HPLC was split between an Agilent 6140 single quad mass spectrometer equipped with a multimode source and an ESA (ESA, Chelmsford, MA) Corona charged aerosol detector. HPLC reversed-phase separations were performed on a 50 × 2-mm Kinetex 2.6- μ m C18 column (Phenomenex, Torrance, CA) at a flow rate of 700 μ L per minute using a gradient comprising (A) HPLC grade water (VWR) with 0.05% formic acid (Sigma Aldrich) and (B) HPLC grade acetonitrile (Honeywell) with 0.05% formic acid. The conditions for pump 1 were at time 0, A = 90%, with a linear gradient such that after 2 min, B = 100%, which was held for 0.5 min before returning to starting conditions. The gradient conditions for pump 2 were the opposite of pump 1 so as to combine the 2 solvent streams after the column and produce a constant 50:50 volume/volume mix of A and B at the detectors. The Agilent 6140 MS acquired from 100 to 1000 Da in sequential positive and negative ion modes with a total cycle time of 1 s, and the output from the Corona CAD (ESA) detector was acquired at a rate of 5 Hz through the analog-to-digital converter. The diode array detector (DAD) scanned from 220 to 300 nm at a rate of 20 Hz. All data were acquired into Chemstation Version B.03.01 (Agilent). The data from the DAD and CAD detectors were integrated automatically within Chemstation.

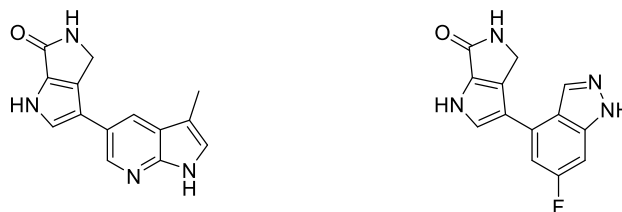
Compound	Purity (%)
S1	100
1	100
2	97.8
3	100
4	100
5	96.3
6	100
7	98.4
8	97.8
9	97.4

Source of compounds 1, 2 and S1.

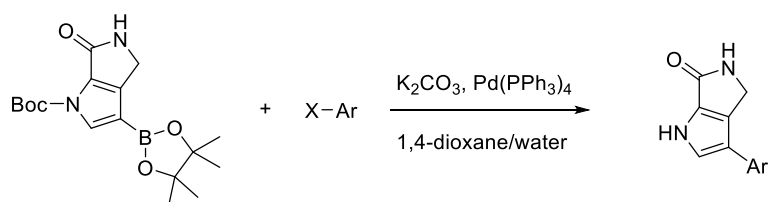
Compounds S1 and 1 are commercially available. Compound 2 can be prepared following published procedures.¹⁵⁻

17

Synthesis of compounds 3 and 4



3-(3-methyl-1H-pyrrolo[2,3-b]pyridin-5-yl)-4,5-dihydropyrrolo[3,4-b]pyrrol-6(1H)-one (**compound 3**) and 3-(6-fluoro-1H-indazol-4-yl)-4,5-dihydropyrrolo[3,4-b]pyrrol-6(1H)-one (**compound 4**) were synthesised in a library format using the general procedure detailed below.

General procedure:

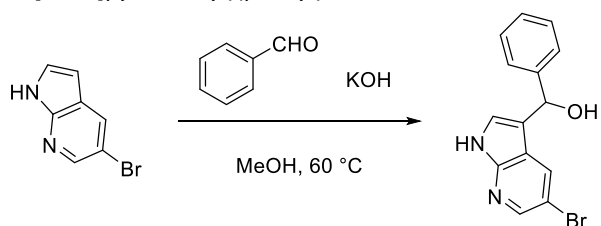
$Pd(PPh_3)_4$ (0.014 mmol, 0.01 equiv) was added in one portion to a mixture of *tert*-butyl 6-oxo-3-(4,4,5,5-tetramethyl-1,3,2-dioxaborolan-2-yl)-5,6-dihydropyrrolo[3,4-*b*]pyrrole-1(4*H*)-carboxylate¹⁸ (0.14 mmol, 1.0 equiv), halogen-containing reagent (0.21 mmol, 1.5 equiv), K_2CO_3 (0.42 mmol, 3.0 equiv) in 1,4-dioxane (2 mL) and H_2O (0.5 mL) under N_2 at rt. The mixture was stirred at 100 °C for 16 h.^a The crude product was purified by preparative HPLC (Shim-pack XR-ODS, 2.2 μm , 4.6 x 50 mm) using decreasingly polar mixtures of water (containing 0.05% TFA) and MeCN as eluents (elution gradient 5 to 100%) to afford the product.

Compound	Name	Halogen-containing reagent	Synthesised amount (mg)	Yield (%)	m/z (ES+), [M+H] ⁺	Purity (%)
3	3-(3-methyl-1 <i>H</i> -pyrrolo[2,3- <i>b</i>]pyridin-5-yl)-4,5-dihydropyrrolo[3,4- <i>b</i>]pyrrol-6(1 <i>H</i>)-one		4.1	12	253.1	100
4	3-(6-fluoro-1 <i>H</i> -indazol-4-yl)-4,5-dihydropyrrolo[3,4- <i>b</i>]pyrrol-6(1 <i>H</i>)-one		2.3	6	257.1	100

^a The -Boc group was cleaved *in situ*.

Synthesis of compound 5

Synthesis of (5-bromo-1H-pyrrolo[2,3-b]pyridin-3-yl)(phenyl)methanol:

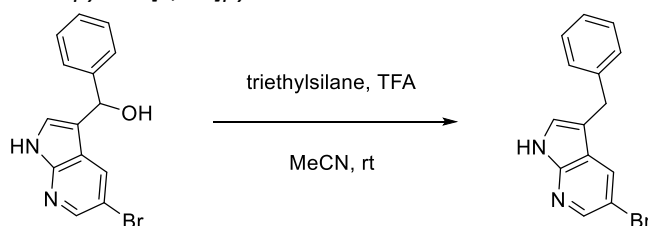


To a solution of 5-bromo-1H-pyrrolo[2,3-b]pyridine (5.00 g, 25.4 mmol), benzaldehyde (2.69 g, 25.4 mmol) in MeOH (30 mL), was added KOH (4.27 g, 76.1 mmol) at rt. The resulting mixture was heated at 60 °C for 12 hours. The reaction mixture was neutralised using 2M HCl and concentrated under reduced pressure to remove the MeOH. Subsequently, the residue was diluted with EtOAc (100 mL) and washed with brine (2 x 30 mL). The organic layer was dried over anhydrous Na₂SO₄, filtered and concentrated under reduced pressure. The crude product was purified by flash column chromatography (elution gradient 0 to 50% EtOAc in petroleum ether). Pure fractions were evaporated to dryness to afford (5-bromo-1H-pyrrolo[2,3-b]pyridin-3-yl)(phenyl)methanol (1.90 g, 25 % yield) as a white solid.

¹H NMR (300 MHz, DMSO-d₆) δ 5.79 (s, 1H), 5.92 (s, 1H), 7.20-7.46 (m, 6H), 7.96 (d, *J* = 2.3 Hz, 1H), 8.20 (d, *J* = 2.3 Hz, 1H), 11.76 (s, 1H)

m/z (ES+), [M+H]⁺ = 303.0

Synthesis of 3-benzyl-5-bromo-1H-pyrrolo[2,3-b]pyridine:

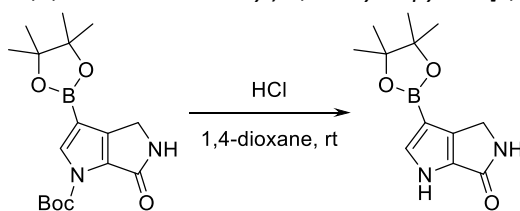


To a solution of (5-bromo-1H-pyrrolo[2,3-b]pyridin-3-yl)(phenyl)methanol (1.30 g, 4.29 mmol) in MeCN (50 mL), was added TFA (994 μL, 12.9 mmol) and triethylsilane (1.50 g, 12.9 mmol) at rt under N₂. The resulting mixture was stirred at rt for 12 hours. The reaction mixture was concentrated under reduced pressure and the residue dried under high vacuum to remove the residual TFA. The crude product was re-dissolved with 30 mL of ammonia solution (7M in MeOH) and then concentrated under reduced pressure. The crude product was purified by flash column chromatography (elution gradient 0 to 50% EtOAc in petroleum ether). Pure fractions were evaporated to dryness to afford 3-benzyl-5-bromo-1H-pyrrolo[2,3-b]pyridine (500 mg, 41 % yield) as a white solid.

¹H NMR (300 MHz, DMSO-d₆) δ 4.01 (s, 2H), 7.09 – 7.18 (m, 1H), 7.22 – 7.31 (m, 4H), 7.37 (d, *J* = 2.5 Hz, 1H), 8.01 (dd, *J* = 2.3, 0.7 Hz, 1H), 8.21 (dd, *J* = 5.0, 2.2 Hz, 1H), 11.69 (s, 1H)

m/z (ES+), [M+H]⁺ = 287.1

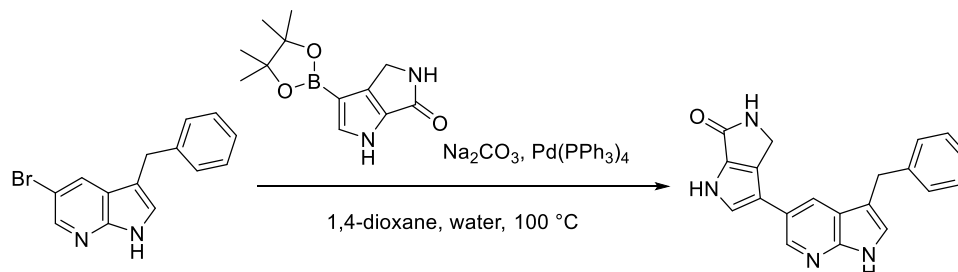
Synthesis of 3-(4,4,5,5-tetramethyl-1,3,2-dioxaborolan-2-yl)-4,5-dihydropyrrolo[3,4-b]pyrrol-6(1H)-one:



Tert-butyl 6-oxo-3-(4,4,5,5-tetramethyl-1,3,2-dioxaborolan-2-yl)-5,6-dihydropyrrolo[3,4-*b*]pyrrole-1(4*H*)-carboxylate¹⁸ (400 mg, 1.15 mmol) was added in one portion to a solution of HCl in 1,4-dioxane (4*M*, 5.00 mL, 20.0 mmol) under N₂. The resulting solution was stirred at rt for 3 hours before the mixture was evaporated to dryness to afford 3-(4,4,5,5-tetramethyl-1,3,2-dioxaborolan-2-yl)-4,5-dihydropyrrolo[3,4-*b*]pyrrol-6(1*H*)-one (280 mg, 98 %) as a pale yellow solid. The afforded material was carried over to the next-step without any further purification.

m/z (ES⁺), [M+H]⁺ = 249.1

*Synthesis of 3-(3-benzyl-1*H*-pyrrolo[2,3-*b*]pyridin-5-yl)-4,5-dihydropyrrolo[3,4-*b*]pyrrol-6(1*H*)-one (compound 5):*



To a degassed suspension of 3-benzyl-5-bromo-1*H*-pyrrolo[2,3-*b*]pyridine (500 mg, 1.74 mmol), 3-(4,4,5,5-tetramethyl-1,3,2-dioxaborolan-2-yl)-4,5-dihydropyrrolo[3,4-*b*]pyrrol-6(1*H*)-one (518 mg, 2.09 mmol) and Na₂CO₃ (554 mg, 5.22 mmol) in 1,4-dioxane (10 mL) and water (5.0 mL) was added Pd(PPh₃)₄ (201 mg, 0.174 mmol) at rt under N₂. The resulting mixture was stirred at 100 °C for 12 hours. The reaction mixture was diluted with EtOAc (80 mL) and washed with brine (2 x 20 mL). The organic layer was dried over anhydrous Na₂SO₄, filtered and concentrated under reduced pressure. The crude product was purified by flash column chromatography (elution gradient 20 to 25% EtOAc in petroleum ether). Pure fractions were evaporated to dryness to afford 3-(3-benzyl-1*H*-pyrrolo[2,3-*b*]pyridin-5-yl)-4,5-dihydropyrrolo[3,4-*b*]pyrrol-6(1*H*)-one (100 mg, 18 % yield) as a yellow solid.

¹H NMR (300 MHz, DMSO-*d*₆) δ 4.05 (s, 2H), 4.30 (s, 2H), 7.12 – 7.21 (m, 1H), 7.23 – 7.31 (m, 3H), 7.32 – 7.40 (m, 2H), 7.53 (d, *J* = 2.4 Hz, 1H), 7.82 (d, *J* = 2.1 Hz, 1H), 7.92 (s, 1H), 8.38 (d, *J* = 2.0 Hz, 1H), 11.34 (s, 1H), 11.76 (s, 1H)

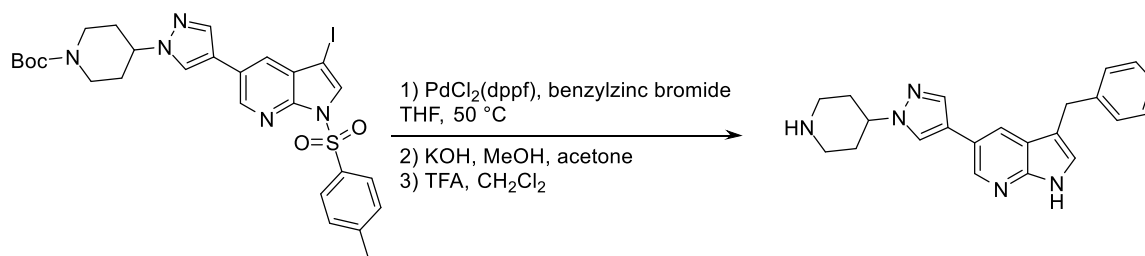
¹³C NMR (75 MHz, DMSO-*d*₆) δ 31.2, 41.6, 113.0, 116.9, 119.3, 122.2, 122.4, 122.6, 123.9, 125.8, 128.3, 128.6, 129.7, 132.3, 140.2, 141.5, 147.4, 163.7

m/z (ES⁺), [M+H]⁺ = 329.2

HRMS (ES⁺) = calculated for [C₂₀H₁₇N₄O]⁺ [M+H]⁺ = 329.1402, found = 329.1417

Synthesis of compound 6

Synthesis of 3-benzyl-5-(1-(piperidin-4-yl)-1H-pyrazol-4-yl)-1H-pyrrolo[2,3-b]pyridine (**compound 6**):



To a degassed mixture of *tert*-butyl 4-(4-(3-iodo-1-tosyl-1H-pyrrolo[2,3-b]pyridin-5-yl)-1H-pyrazol-1-yl)piperidine-1-carboxylate¹⁹ (300 mg, 0.463 mmol) and PdCl₂(dppf) (17.0 mg, 0.0232 mmol), was added a solution of benzylzinc bromide (0.5 M in THF, 4.60 mL, 2.30 mmol) in THF (15 mL) under N₂. The resulting mixture was stirred at 60 °C for 18 hours. The reaction mixture was sequentially quenched with saturated aqueous NH₄Cl and saturated aqueous Na₂(EDTA). The mixture was then partitioned between EtOAc and H₂O and extracted with EtOAc (x2). The combined organic extracts were washed with brine and then dried over anhydrous MgSO₄, filtered and concentrated under reduced pressure. The crude product was purified by flash column chromatography (elution gradient 0 to 1.5% MeOH in CH₂Cl₂). Fractions containing the desired product were evaporated to dryness to provide a yellow solid (244 mg). This material was dissolved in MeOH/acetone (3.0 mL, 1:1) before the addition of 50% aqueous KOH (1.1 mL). The mixture was stirred at rt for 20 min and subsequently acidified to pH 4 using 2M HCl (aq). The mixture was then partitioned between EtOAc and H₂O and extracted with EtOAc (x2). The combined organic extracts were washed with brine and then dried over anhydrous MgSO₄, filtered and concentrated under reduced pressure. The crude material was dissolved in CH₂Cl₂/TFA (3.0 mL, 3:1) and stirred at rt for 1 hour. The reaction mixture was concentrated under reduced pressure and purified by preparative HPLC. Pure fractions were evaporated to dryness to afford 3-benzyl-5-(1-(piperidin-4-yl)-1H-pyrazol-4-yl)-1H-pyrrolo[2,3-b]pyridine as a white solid (57.5 mg, 35% over 3-steps).

¹H NMR (500 MHz, DMSO-d₆) δ 1.85 (qd, *J* = 12.0, 3.7 Hz, 2H), 2.00 (d, *J* = 10.6 Hz, 2H), 2.64 (t, *J* = 11.6 Hz, 2H), 3.08 (d, *J* = 12.2 Hz, 2H), 4.05 (s, 2H), 4.17 – 4.26 (m, 1H), 7.11 – 7.19 (m, 1H), 7.21 – 7.30 (m, 3H), 7.32 (d, *J* = 7.3 Hz, 2H), 7.86 (s, 1H), 8.00 – 8.04 (m, 1H), 8.20 (s, 1H), 8.44 – 8.47 (m, 1H), 11.37 (s, 1H)

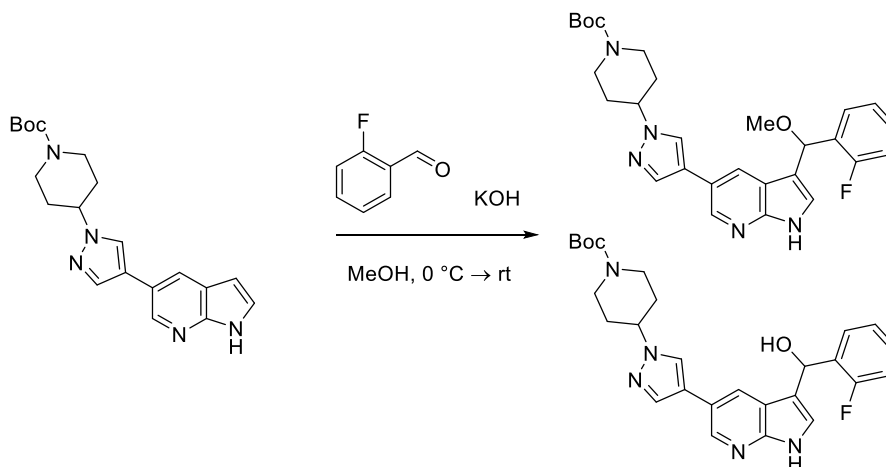
¹³C NMR (125 MHz, DMSO-d₆) δ 30.9, 33.1, 44.8, 58.8, 112.8, 119.3, 119.9, 120.3, 122.7, 124.0, 124.3, 125.7, 128.3, 128.4, 135.4, 140.4, 141.4, 147.6

m/z (ES⁺), [M+H]⁺ = 358.7

HRMS (ES⁺) = calculated for [C₂₂H₂₄N₅]⁺ [M+H]⁺ = 358.2032, found = 358.2038

Synthesis of compound 7

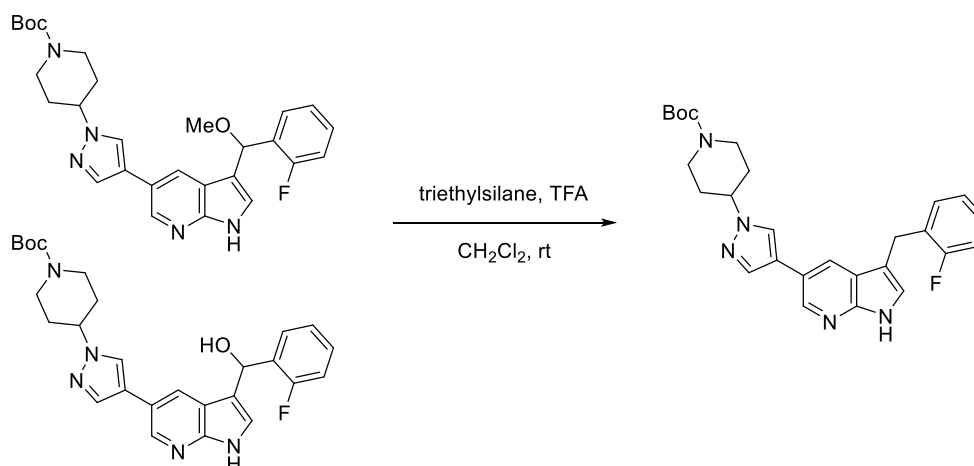
Synthesis of *tert*-butyl 4-(4-(3-((2-fluorophenyl)(methoxy)methyl)-1*H*-pyrrolo[2,3-*b*]pyridin-5-yl)-1*H*-pyrazol-1-yl)piperidine-1-carboxylate:



To a solution of *tert*-butyl 4-(4-(1*H*-pyrrolo[2,3-*b*]pyridin-5-yl)-1*H*-pyrazol-1-yl)piperidine-1-carboxylate¹⁹ (426 mg, 1.16 mmol) and 2-fluorobenzaldehyde (252 μ L, 2.38 mmol) in MeOH (2.7 ml) at 0 °C, was added KOH (800 mg, 14.3 mmol) in one portion. The reaction was allowed to warm to rt. After 7 hours, the white mixture was poured into EtOAc and washed successively with 50% and 100% saturated aqueous NaCl. The organic layer was dried over anhydrous Na₂SO₄, filtered and concentrated under reduced pressure. The crude product was purified by flash column chromatography (elution gradient 50 to 100% EtOAc in hexanes). Fractions containing the desired product were evaporated to dryness to afford *tert*-butyl 4-(4-(3-((2-fluorophenyl)(methoxy)methyl)-1*H*-pyrrolo[2,3-*b*]pyridin-5-yl)-1*H*-pyrazol-1-yl)piperidine-1-carboxylate contaminated with the closely eluting *tert*-butyl 4-(4-(3-((2-fluorophenyl)(hydroxy)methyl)-1*H*-pyrrolo[2,3-*b*]pyridin-5-yl)-1*H*-pyrazol-1-yl)piperidine-1-carboxylate (242 mg, 83:17 mixture by NMR) as a white solid. The afforded material was carried over to the next-step without any further purification.

m/z (ES⁺), [M+H]⁺ = 506.2 (methoxy); 492.2 (hydroxy)

Synthesis of *tert*-butyl 4-(4-(3-(2-fluorobenzyl)-1*H*-pyrrolo[2,3-*b*]pyridin-5-yl)-1*H*-pyrazol-1-yl)piperidine-1-carboxylate:



To a solution of impure *tert*-butyl 4-(4-(3-((2-fluorophenyl)(methoxy)methyl)-1*H*-pyrrolo[2,3-*b*]pyridin-5-yl)-1*H*-pyrazol-1-yl)piperidine-1-carboxylate (242 mg, 0.479 mmol)^b in CH₂Cl₂ (3.6 mL) was added sequentially triethylsilane (917 μ L, 5.74 mmol) and TFA (295 μ L, 3.83 mmol). The resulting yellow solution was stirred at rt for 1.5 hours before being quenched with saturated aqueous NaHCO₃ (aq). The mixture was extracted with EtOAc and the organic layer

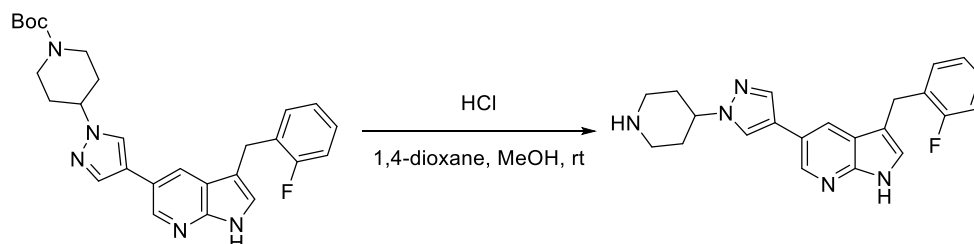
^b Material assumed pure for the purposes of reagent equivalent calculation.

was dried over anhydrous Na₂SO₄, filtered and concentrated under reduced pressure. The crude product was purified by flash column chromatography (elution gradient 80 to 100% EtOAc in hexanes). Pure fractions were evaporated to dryness to afford *tert*-butyl 4-(4-(3-(2-fluorobenzyl)-1*H*-pyrrolo[2,3-*b*]pyridin-5-yl)-1*H*-pyrazol-1-yl)piperidine-1-carboxylate (187 mg, 34% over two-steps) as a white foam solid.

¹H NMR (300 MHz, DMSO-*d*₆) δ 1.43 (s, 9H), 1.82 (qd, *J* = 12.3, 4.4 Hz, 2H), 1.99 – 2.11 (m, 2H), 2.80 – 3.08 (m, 2H), 3.98 – 4.13 (m, 4H), 4.37 (tt, *J* = 11.4, 3.8 Hz, 1H), 7.01 – 7.40 (m, 5H), 7.86 – 7.89 (m, 1H), 8.04 (d, *J* = 2.0 Hz, 1H), 8.25 (s, 1H), 8.46 (d, *J* = 2.1 Hz, 1H), 11.34 – 11.42 (m, 1H)

m/z (ES+), [M+H]⁺ = 476.2

*Synthesis of 3-(2-fluorobenzyl)-5-(1-(piperidin-4-yl)-1*H*-pyrazol-4-yl)-1*H*-pyrrolo[2,3-*b*]pyridine (compound 7):*



To a solution of *tert*-butyl 4-(4-(3-(2-fluorobenzyl)-1*H*-pyrrolo[2,3-*b*]pyridin-5-yl)-1*H*-pyrazol-1-yl)piperidine-1-carboxylate (170 mg, 0.357 mmol) in MeOH (1.0 mL) was added HCl in 1,4-dioxane (4M, 3.00 mL, 12.0 mmol) at rt. After 15 min, the light yellow solution was concentrated under reduced pressure to an off-white solid (170 mg, ~93% pure by LCMS). 64 mg of the crude material were purified by preparative HPLC (XB-C18, 100 Å, 5 μm, 4.6 x 50 mm) using decreasingly polar mixtures of water (containing 0.2% NH₄OH, pH 10) and MeCN as eluents (elution gradient 30 to 50%) to afford 3-(2-fluorobenzyl)-5-(1-(piperidin-4-yl)-1*H*-pyrazol-4-yl)-1*H*-pyrrolo[2,3-*b*]pyridine (37.0 mg, 28 %) as a white solid.

¹H NMR (500 MHz, DMSO-*d*₆) δ 1.81 (qd, *J* = 12.1, 4.0 Hz, 2H), 1.94 – 2.01 (m, 2H), 2.59 (td, *J* = 12.3, 2.0 Hz, 2H), 3.00 – 3.09 (m, 2H), 4.08 (s, 2H), 4.18 (tt, *J* = 11.5, 4.0 Hz, 1H), 7.10 (td, *J* = 7.4, 1.2 Hz, 1H), 7.13 – 7.27 (m, 3H), 7.32 (td, *J* = 7.8, 1.6 Hz, 1H), 7.84 – 7.88 (m, 1H), 8.05 (d, *J* = 2.0 Hz, 1H), 8.20 (s, 1H), 8.47 (d, *J* = 2.0 Hz, 1H), 11.39 (s, 1H)

¹³C NMR (125 MHz, DMSO-*d*₆) δ 23.9 (d, *J*_{CF} = 3.4 Hz), 33.6, 45.1, 59.3, 111.1, 115.1 (d, *J*_{CF} = 21.6 Hz), 119.1, 119.8, 120.4, 122.5, 124.2, ^c 124.3 (d, *J*_{CF} = 3.4 Hz), 127.9 (d, *J*_{CF} = 1.6 Hz), 128.0 (d, *J*_{CF} = 5.7 Hz), 130.8 (d, *J*_{CF} = 4.6 Hz), 135.3, 140.5, 147.5, 160.3 (d, *J*_{CF} = 243.5 Hz)

¹⁹F NMR (decoupled) (471 MHz, DMSO-*d*₆) δ -118.3.

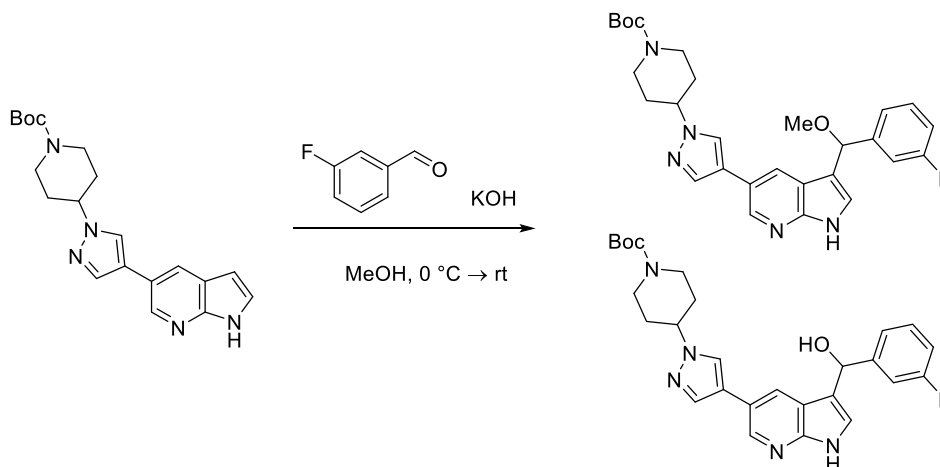
m/z (ES+), [M+H]⁺ = 376.1

HRMS (ES+) = calculated for [C₂₂H₂₃FN₅]⁺ [M+H]⁺ = 376.1937, found = 376.1947

^c This ¹³C peak has two -CH overlaid.

Synthesis of compound 8

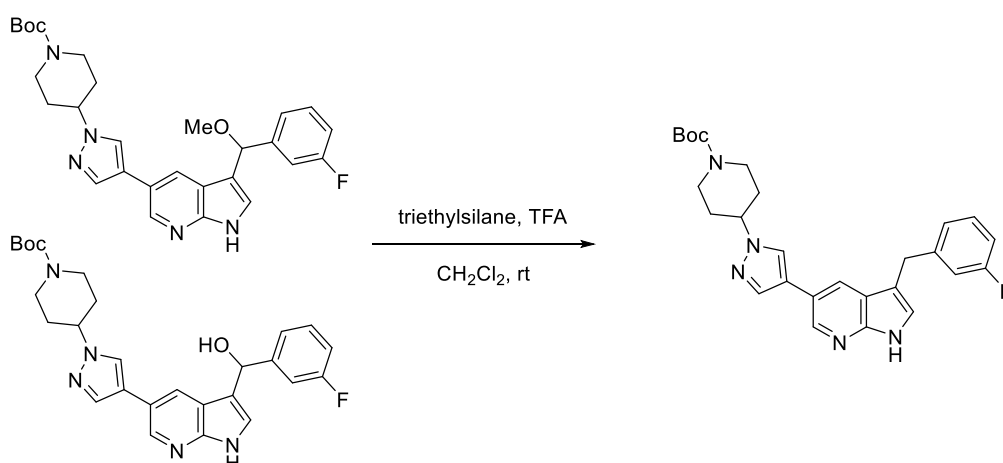
Synthesis of *tert*-butyl 4-(4-(3-((3-fluorophenyl)(methoxy)methyl)-1*H*-pyrrolo[2,3-*b*]pyridin-5-yl)-1*H*-pyrazol-1-yl)piperidine-1-carboxylate:



To a solution of *tert*-butyl 4-(4-(1*H*-pyrrolo[2,3-*b*]pyridin-5-yl)-1*H*-pyrazol-1-yl)piperidine-1-carboxylate (350 mg, 0.953 mmol) and 3-fluorobenzaldehyde (202 μ L, 1.91 mmol) in MeOH (2.2 mL) at 0 °C was added KOH (428 mg, 7.62 mmol) in one portion. The reaction was allowed to warm to rt. After 20 hours, the red-orange solution was poured into EtOAc and washed successively with 50% and 100% saturated aqueous NaCl. The organic layer was dried over anhydrous Na₂SO₄, filtered and concentrated under reduced pressure. The crude product was purified by flash column chromatography (isocratic 100% EtOAc). Fractions containing the desired product were evaporated to dryness to afford *tert*-butyl 4-(4-(3-((3-fluorophenyl)(methoxy)methyl)-1*H*-pyrrolo[2,3-*b*]pyridin-5-yl)-1*H*-pyrazol-1-yl)piperidine-1-carboxylate contaminated with the closely eluting *tert*-butyl 4-(4-(3-((3-fluorophenyl)(hydroxy)methyl)-1*H*-pyrrolo[2,3-*b*]pyridin-5-yl)-1*H*-pyrazol-1-yl)piperidine-1-carboxylate (157 mg, 44:56 by LCMS) as a white solid. The afforded material was carried over to the next-step without any further purification.

m/z (ES⁺), [M+H]⁺ = 506.2 (methoxy); 492.2 (hydroxy)

Synthesis of *tert*-butyl 4-(4-(3-(3-fluorobenzyl)-1*H*-pyrrolo[2,3-*b*]pyridin-5-yl)-1*H*-pyrazol-1-yl)piperidine-1-carboxylate:



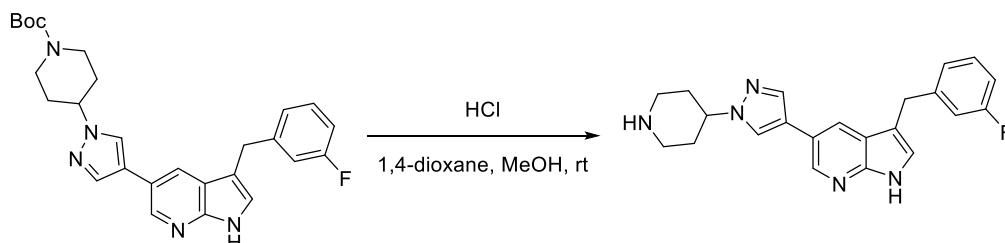
To a solution of impure *tert*-butyl 4-(4-(3-((3-fluorophenyl)(methoxy)methyl)-1*H*-pyrrolo[2,3-*b*]pyridin-5-yl)-1*H*-pyrazol-1-yl)piperidine-1-carboxylate^d (157 mg, 0.311 mmol) in CH₂Cl₂ (5.4 mL) was added sequentially triethylsilane (595 μ L, 3.73 mmol) and TFA (191 μ L, 2.48 mmol) at rt. The resulting yellow solution was stirred at rt for 4 hours

^d Material assumed pure for the purposes of reagent equivalent calculation.

before being quenched with saturated aqueous NaHCO₃. The mixture was extracted with EtOAc and the organic layer was dried over anhydrous Na₂SO₄, filtered and concentrated under reduced pressure. The crude product was purified by flash column chromatography (isocratic 100% EtOAc) to afford *tert*-butyl 4-(4-(3-(3-fluorobenzyl)-1*H*-pyrrolo[2,3-*b*]pyridin-5-yl)-1*H*-pyrazol-1-yl)piperidine-1-carboxylate (117 mg, 26% over two steps) as a light yellow foam solid. The afforded material (~78% pure by LCMS) was carried over to the next-step without any further purification.

m/z (ES⁺), [M+H]⁺ = 476.2

Synthesis of 3-(3-fluorobenzyl)-5-(1-(piperidin-4-yl)-1*H*-pyrazol-4-yl)-1*H*-pyrrolo[2,3-*b*]pyridine (compound 8**):**



To a solution of *tert*-butyl 4-(4-(3-(3-fluorobenzyl)-1*H*-pyrrolo[2,3-*b*]pyridin-5-yl)-1*H*-pyrazol-1-yl)piperidine-1-carboxylate (110 mg, 0.231 mmol) in MeOH (0.5 mL) was added HCl in 1,4-dioxane (4M, 3.00 mL, 12.0 mmol) at rt. After 10 min, the light yellow solution was concentrated under reduced pressure to a white solid (129 mg). 65 mg of the crude material were purified by preparative HPLC (Xbridge Phenyl OBD, 130 Å, 5 μm, 19 x 100 mm) using decreasingly polar mixtures of water (containing 0.2% NH₄OH, pH 10) and MeCN as eluents (elution gradient 30 to 50%) to afford 3-(3-fluorobenzyl)-5-(1-(piperidin-4-yl)-1*H*-pyrazol-4-yl)-1*H*-pyrrolo[2,3-*b*]pyridine (33.0 mg, 38%) as a white solid.

¹H NMR (500 MHz, DMSO-*d*₆) δ 1.80 (qd, *J* = 12.0, 3.9 Hz, 2H), 1.93 – 2.02 (m, 2H), 2.59 (t, *J* = 11.7 Hz, 2H), 3.04 (*d*, *J* = 12.2 Hz, 2H), 4.07 (s, 2H), 4.13 – 4.24 (m, 1H), 6.98 (td, *J* = 8.4, 2.0 Hz, 1H), 7.13 (dt, *J* = 10.3, 2.1 Hz, 1H), 7.17 (*d*, *J* = 7.7 Hz, 1H), 7.26 – 7.35 (m, 2H), 7.83 – 7.89 (m, 1H), 8.05 (*d*, *J* = 2.0 Hz, 1H), 8.20 (s, 1H), 8.46 (*d*, *J* = 2.0 Hz, 1H), 11.40 (s, 1H)

¹³C NMR (125 MHz, DMSO-*d*₆) δ 30.5, 33.6, 45.1, 59.3, 112.1, 112.5 (*d*, *J*_{CF} = 20.9 Hz), 115.0 (*d*, *J*_{CF} = 21.0 Hz), 119.2, 119.8, 120.4, 122.6, 124.2 (*d*, *J*_{CF} = 2.2 Hz), 124.47, 124.49, 130.1 (*d*, *J*_{CF} = 8.4 Hz), 135.3, 140.5, 144.6 (*d*, *J*_{CF} = 7.1 Hz), 147.5, 162.2 (*d*, *J*_{CF} = 243.2 Hz)

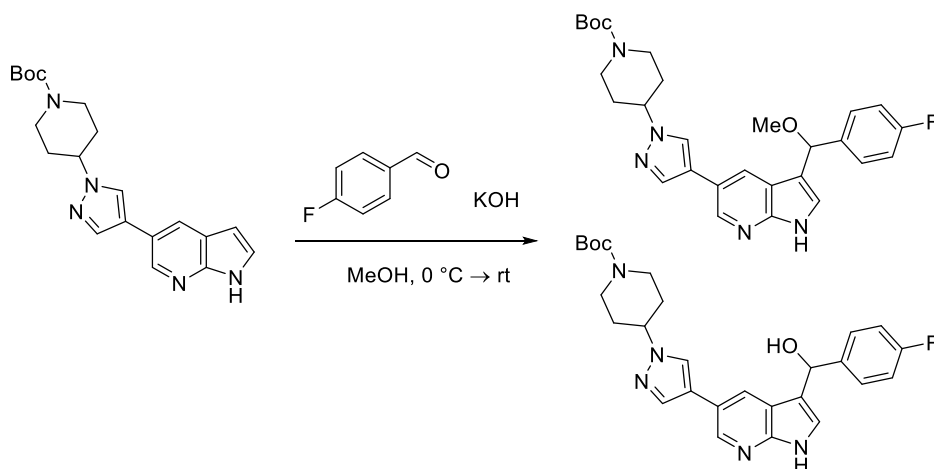
¹⁹F NMR (decoupled) (471 MHz, DMSO-*d*₆) δ -113.7

m/z (ES⁺), [M+H]⁺ = 376.1

HRMS (ES⁺) = calculated for [C₂₂H₂₃FN₅]⁺ [M+H]⁺ = 376.1937, found = 376.1947

Synthesis of compound 9

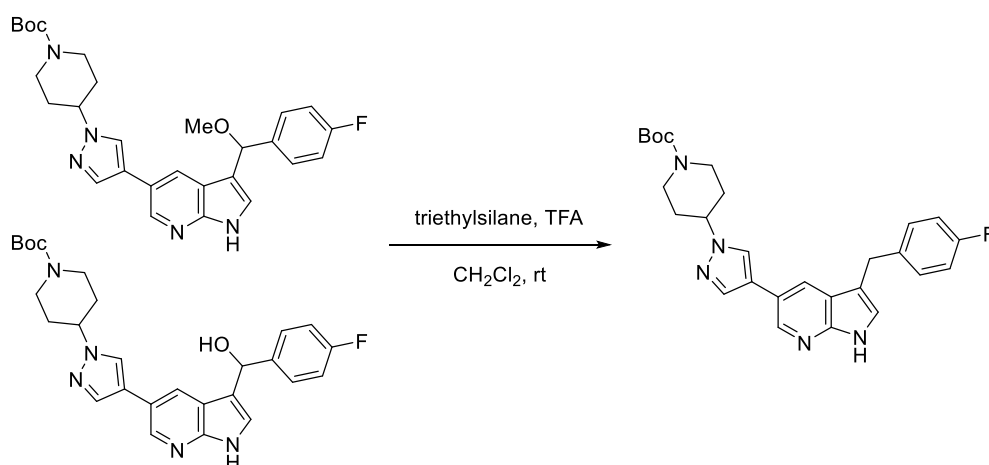
Synthesis of *tert*-butyl 4-(4-(3-((4-fluorophenyl)(methoxy)methyl)-1*H*-pyrrolo[2,3-*b*]pyridin-5-yl)-1*H*-pyrazol-1-yl)piperidine-1-carboxylate :



To a solution of *tert*-butyl 4-(4-(1*H*-pyrrolo[2,3-*b*]pyridin-5-yl)-1*H*-pyrazol-1-yl)piperidine-1-carboxylate¹⁹ (260 mg, 0.708 mmol) and 4-fluorobenzaldehyde (152 μ L, 1.42 mmol) in MeOH (1.6 mL) at 0 $^{\circ}$ C was added KOH (318 mg, 5.66 mmol) in one portion. The reaction was allowed to warm to rt. After 20 hours, the red-orange solution was poured into EtOAc and washed successively with 50% and 100% saturated aqueous NaCl. The organic layer was dried over anhydrous Na₂SO₄, filtered and concentrated under reduced pressure. The crude product was purified by flash column chromatography (elution gradient 80 to 100% EtOAc in hexanes). Fractions containing the desired product were evaporated to dryness to afford *tert*-butyl 4-(4-(3-((4-fluorophenyl)(methoxy)methyl)-1*H*-pyrrolo[2,3-*b*]pyridin-5-yl)-1*H*-pyrazol-1-yl)piperidine-1-carboxylate contaminated with the closely eluting *tert*-butyl 4-(4-(3-((4-fluorophenyl)(hydroxy)methyl)-1*H*-pyrrolo[2,3-*b*]pyridin-5-yl)-1*H*-pyrazol-1-yl)piperidine-1-carboxylate (120 mg, 40:60 by LCMS) as a white solid. The afforded material was carried over to the next-step without any further purification.

m/z (ES⁺), [M+H]⁺ = 506.2 (methoxy); 492.2 (hydroxy)

Synthesis of *tert*-butyl 4-(4-(3-(4-fluorobenzyl)-1*H*-pyrrolo[2,3-*b*]pyridin-5-yl)-1*H*-pyrazol-1-yl)piperidine-1-carboxylate:



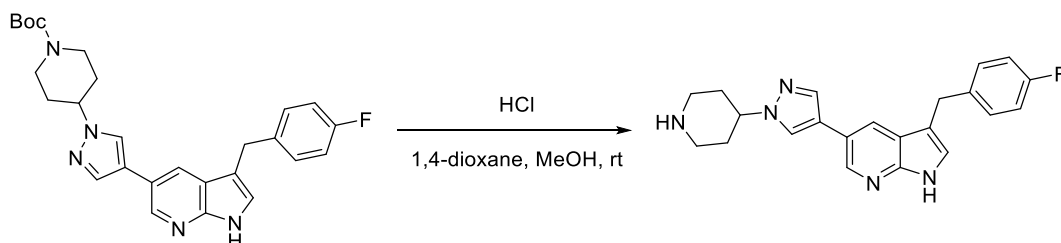
To a solution of impure *tert*-butyl 4-(4-(3-((4-fluorophenyl)(methoxy)methyl)-1*H*-pyrrolo[2,3-*b*]pyridin-5-yl)-1*H*-pyrazol-1-yl)piperidine-1-carboxylate^e (120 mg, 0.237 mmol) in CH₂Cl₂ (3.2 ml) was added sequentially triethylsilane (351 μ L, 2.20 mmol) and TFA (113 μ L, 1.46 mmol) at rt. The resulting mixture was stirred at rt for 5 hours before being quenched with saturated aqueous NaHCO₃. The mixture was extracted with EtOAc and the organic layer was dried

^e Material assumed pure for the purposes of reagent equivalent calculation.

over anhydrous Na₂SO₄, filtered and concentrated under reduced pressure. The crude product was purified by flash column chromatography (elution gradient 80 to 100% EtOAc in hexanes) to afford impure *tert*-butyl 4-(4-(3-(4-fluorobenzyl)-1*H*-pyrrolo[2,3-*b*]pyridin-5-yl)-1*H*-pyrazol-1-yl)piperidine-1-carboxylate (108 mg, 57% pure by LCMS) as a white foam solid. The afforded material was carried over to the next-step without any further purification.

m/z (ES+), [M+H]⁺ = 476.2

Synthesis of 3-(4-fluorobenzyl)-5-(1-(piperidin-4-yl)-1*H*-pyrazol-4-yl)-1*H*-pyrrolo[2,3-*b*]pyridine (compound 9**):**



To a solution of impure *tert*-butyl 4-(4-(3-(4-fluorobenzyl)-1*H*-pyrrolo[2,3-*b*]pyridin-5-yl)-1*H*-pyrazol-1-yl)piperidine-1-carboxylate^e (108 mg) in MeOH (0.5 mL) was added HCl in 1,4-dioxane (4M, 3.00 mL, 12.0 mmol) at rt. After 10 min, the light yellow solution was concentrated under reduced pressure to a light yellow foam. The crude material was purified by preparative HPLC (XB-C18, 100 Å, 5 μm, 4.6 x 50 mm) using decreasingly polar mixtures of water (containing 0.2% NH₄OH, pH 10) and MeOH as eluents (elution gradient 55 to 70%) to afford 3-(4-fluorobenzyl)-5-(1-(piperidin-4-yl)-1*H*-pyrazol-4-yl)-1*H*-pyrrolo[2,3-*b*]pyridine (22.0 mg, 8% over 3-steps) as a white solid.

¹H NMR (500 MHz, DMSO-*d*₆) δ 1.80 (qd, *J* = 12.1, 4.1 Hz, 2H), 1.94 – 2.01 (m, 2H), 2.54 (s, 1H), 2.59 (td, *J* = 12.4, 2.3 Hz, 2H), 3.01 – 3.08 (m, 2H), 4.04 (s, 2H), 4.18 (tt, *J* = 11.6, 4.0 Hz, 1H), 7.05 – 7.12 (m, 2H), 7.24 (s, 1H), 7.34 (ddd, *J* = 8.6, 5.4, 2.6 Hz, 2H), 7.85 (d, *J* = 0.7 Hz, 1H), 8.02 (d, *J* = 2.1 Hz, 1H), 8.17 – 8.22 (m, 1H), 8.45 (d, *J* = 2.1 Hz, 1H), 11.36 (s, 1H)

¹³C NMR (125 MHz, DMSO-*d*₆) δ 30.0, 33.7, 45.2, 59.3, 112.7, 114.9 (d, *J*_{CF} = 21.1 Hz), 119.1, 119.8, 120.4, 122.6, 124.0, 124.2, 130.1 (d, *J*_{CF} = 8.1 Hz), 135.3, 137.6 (d, *J*_{CF} = 3.3 Hz), 140.4, 147.6, 160.6 (d, *J*_{CF} = 241.1 Hz)

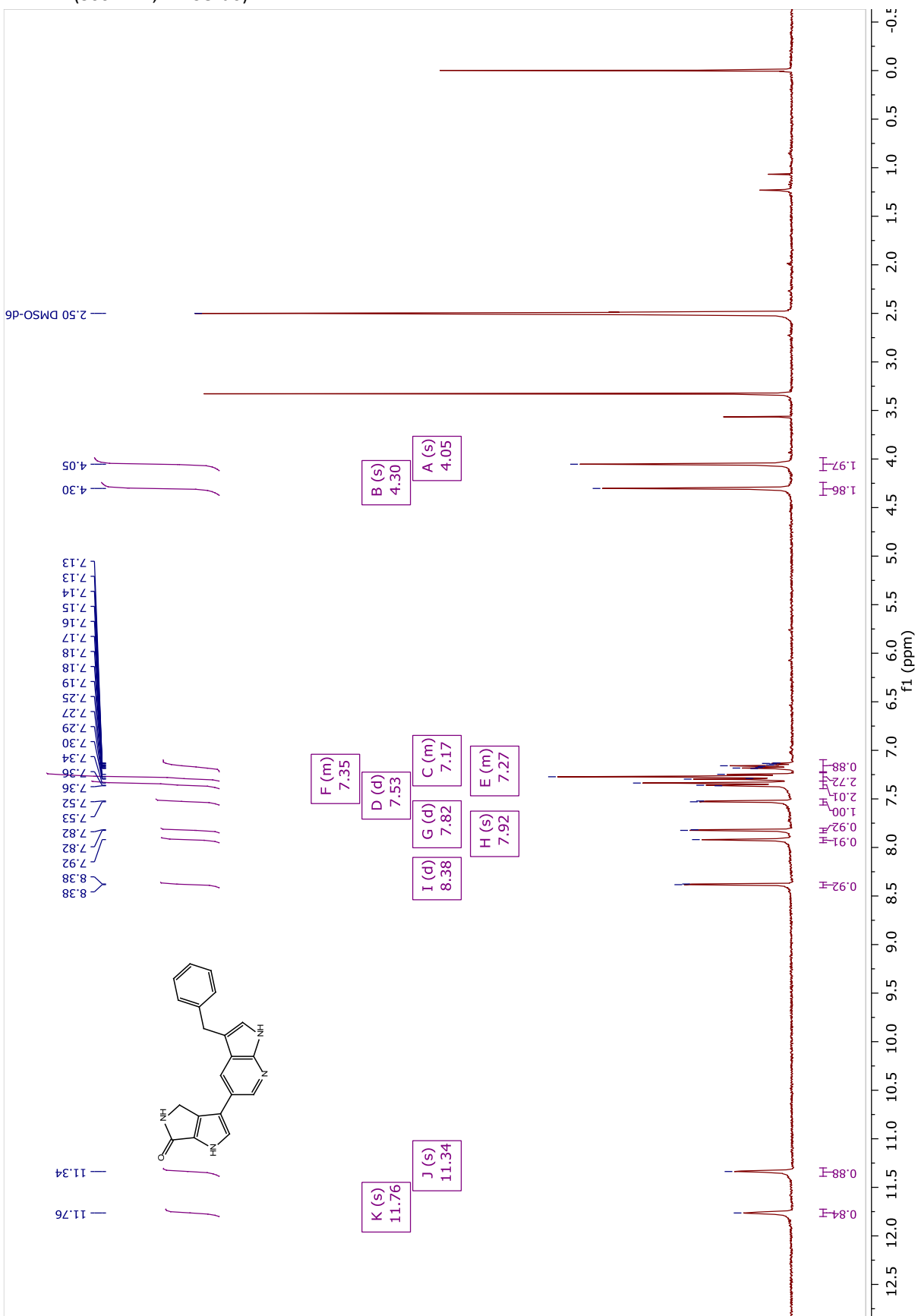
¹⁹F NMR (decoupled) (471 MHz, DMSO-*d*₆) δ -117.7

m/z (ES+), [M+H]⁺ = 376.1

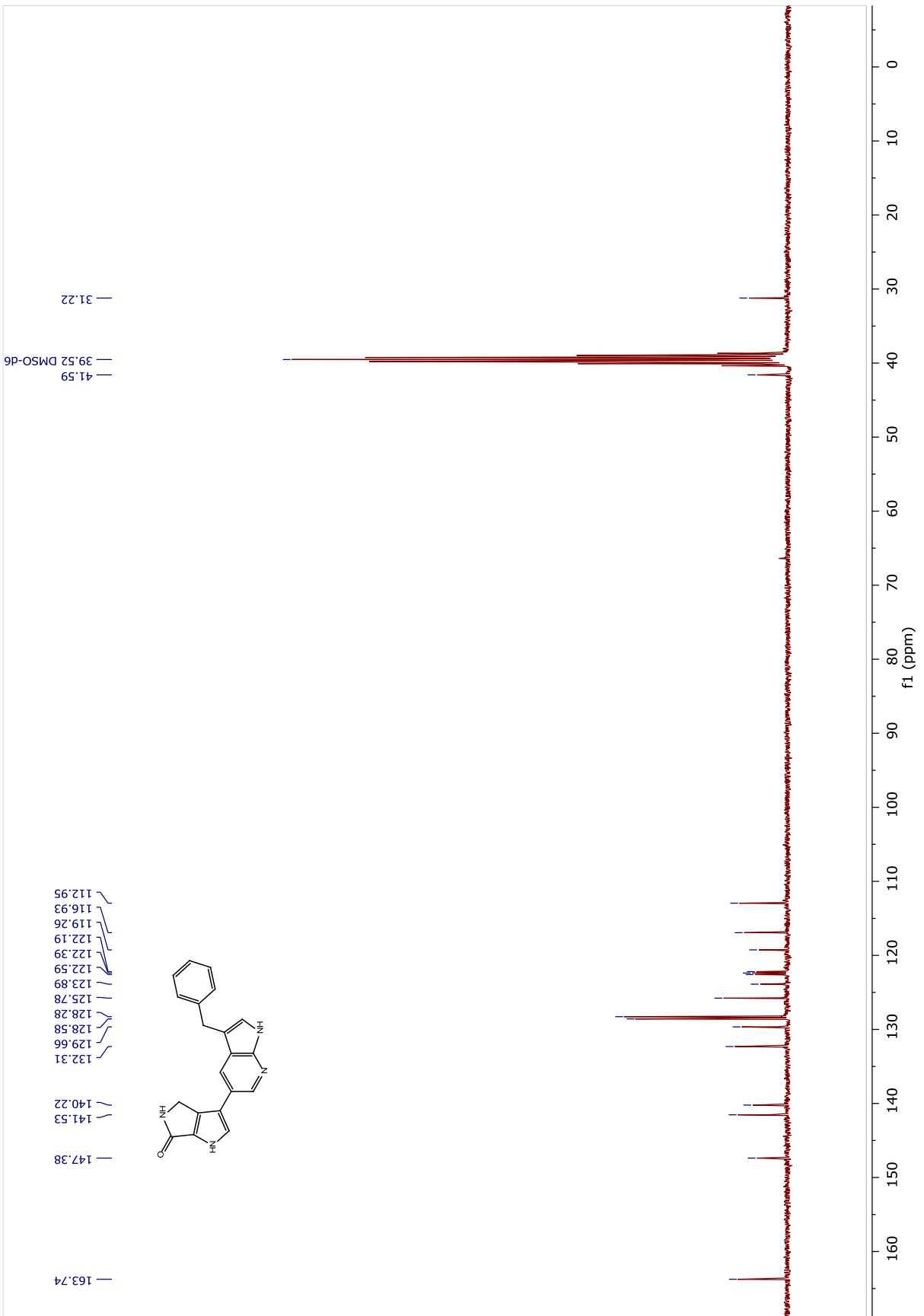
HRMS (ES+) = calculated for [C₂₂H₂₃FN₅]⁺ [M+H]⁺ = 376.1937, found = 376.1947

NMR spectra for compound 5:

¹H NMR (300 MHz, DMSO-d6)

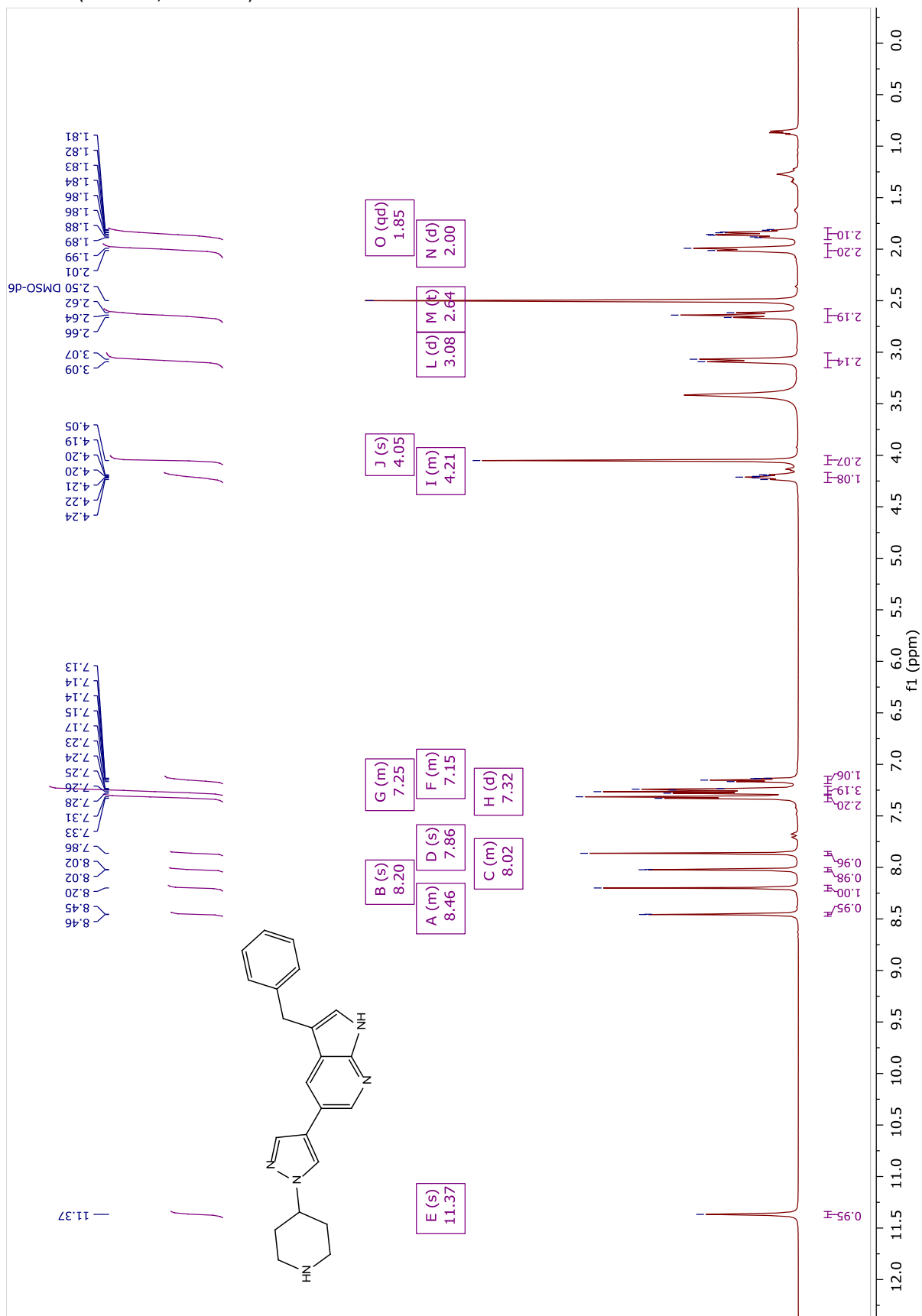


¹³C NMR (75 MHz, DMSO-d6)

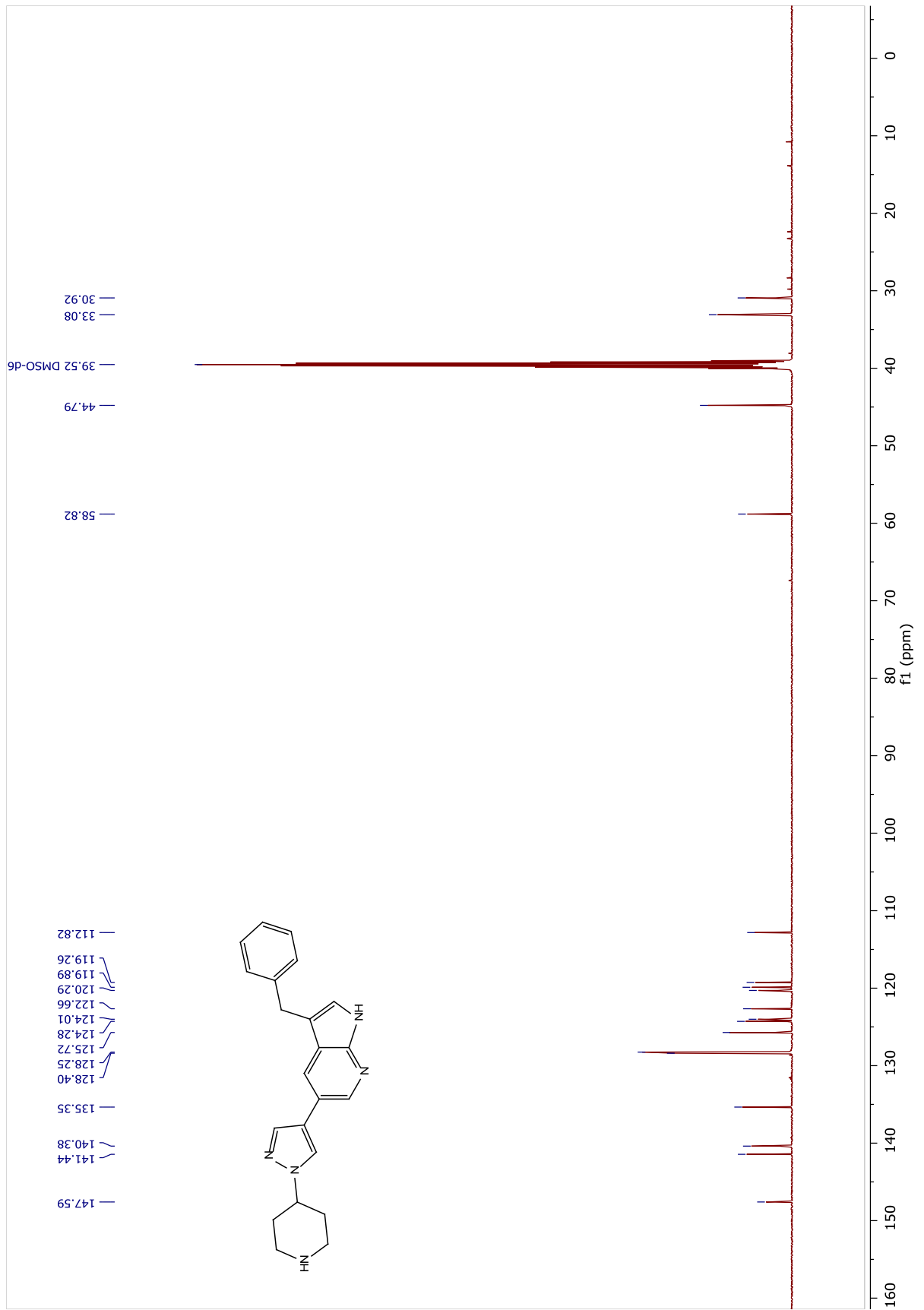


NMR spectra for compound 6:

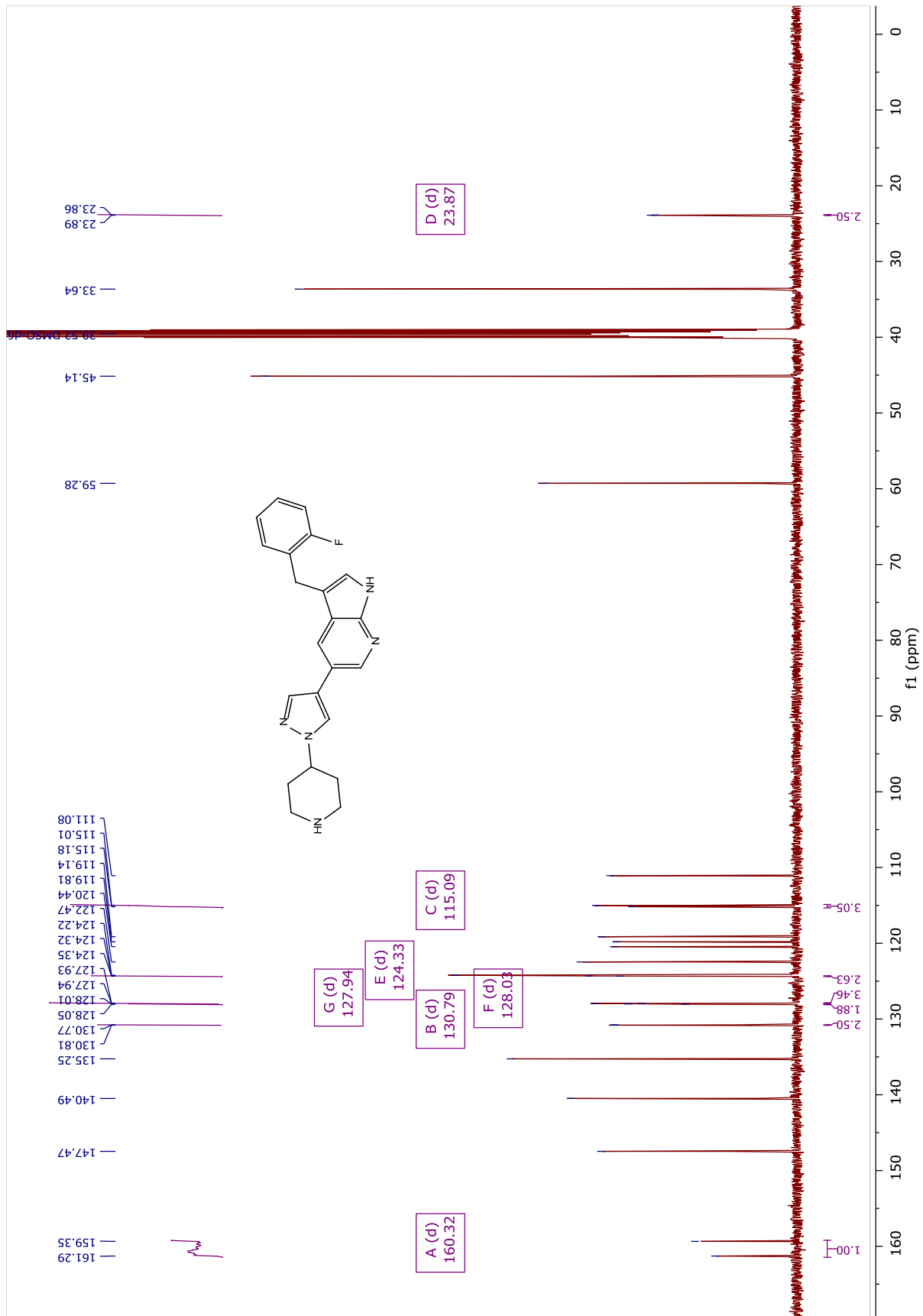
¹H NMR (500 MHz, DMSO-d₆)



¹³C NMR (125 MHz, DMSO-d6)

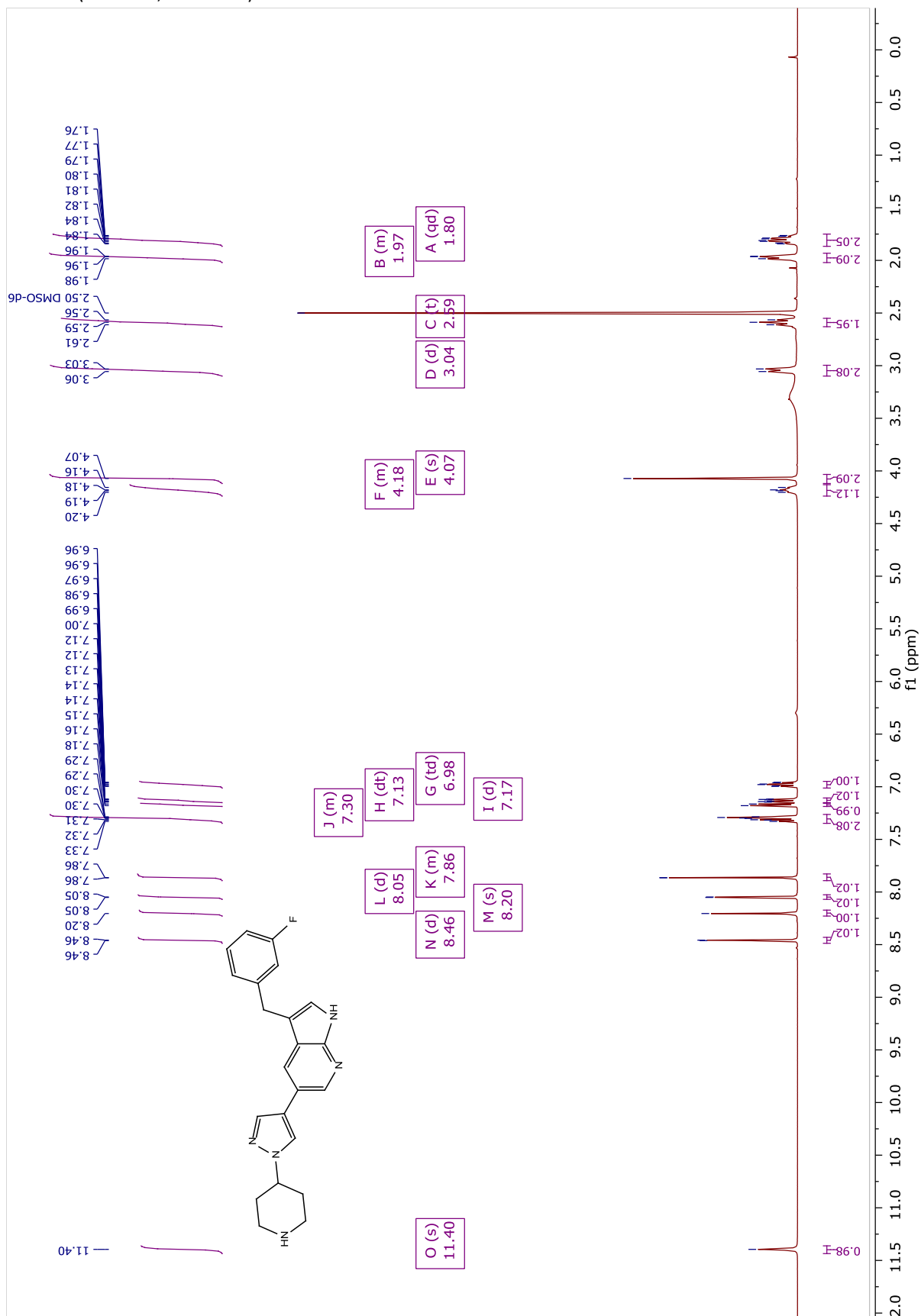


¹³C NMR (125 MHz, DMSO-d6)

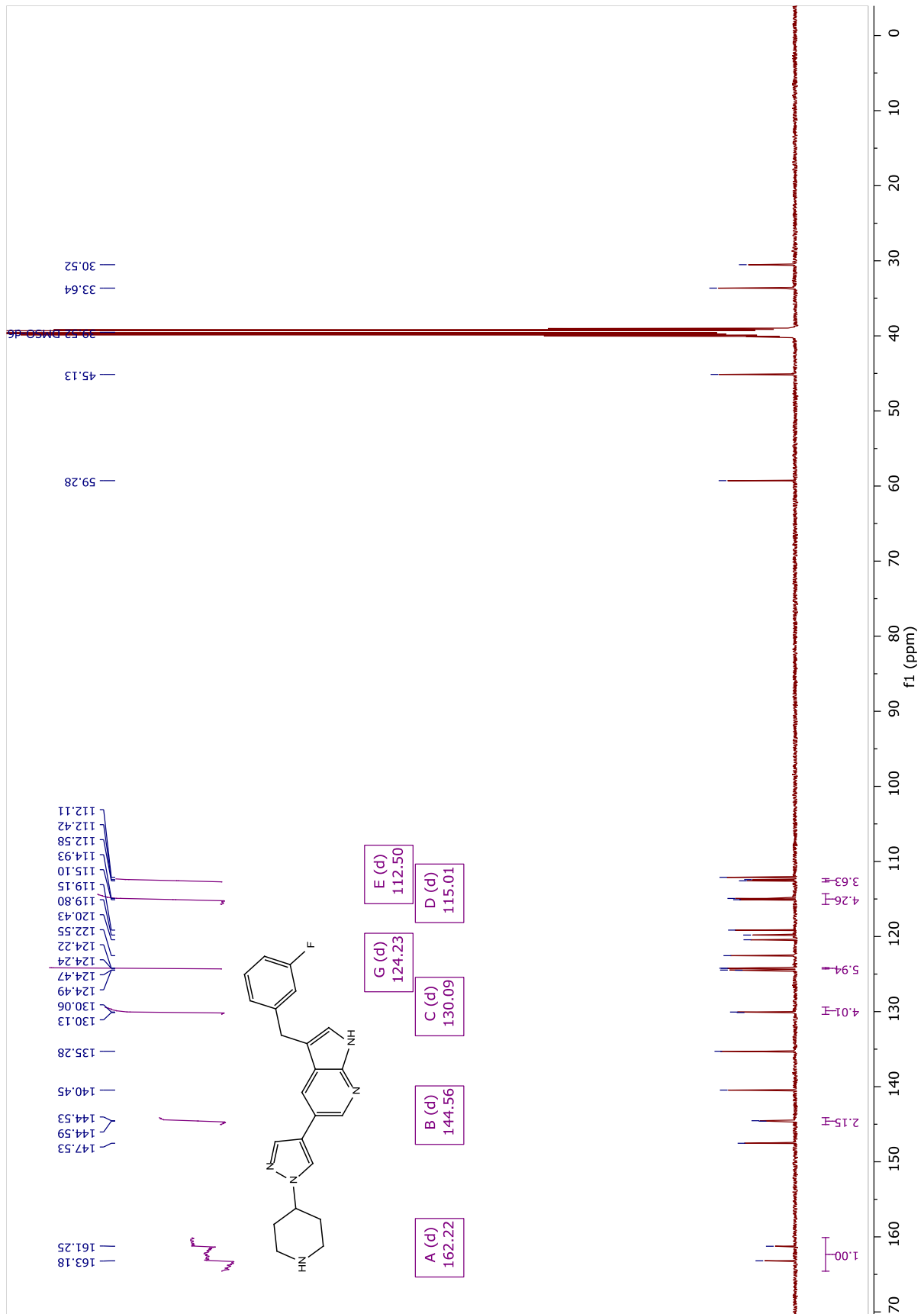


NMR spectra for compound 8:

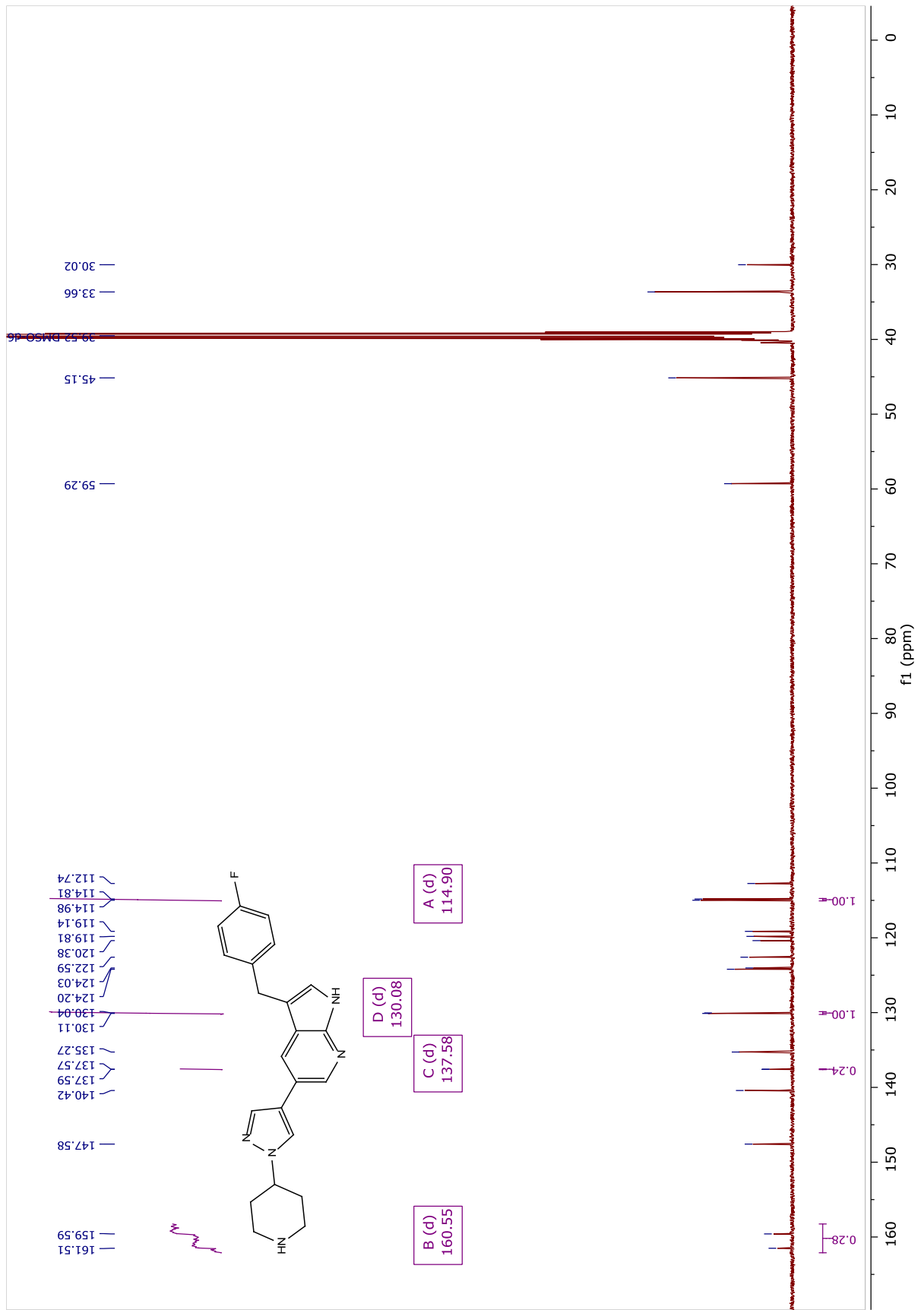
¹H NMR (500 MHz, DMSO-d6)



¹³C NMR (125 MHz, DMSO-d6)



¹³C NMR (125 MHz, DMSO-d6)



Chemistry abbreviations

°C	Degrees Celsius
Ac	Acetyl
App	Apparent
Aq	Aqueous
Ar	Aryl
Bn	Benzyl
Boc	<i>tert-butoxycarbonyl</i>
Bp	Boiling point
br	Broad
D	Doublet
dd	Doublet of doublets
DMF	Dimethylformamide
DMSO	Dimethyl sulfoxide
Dppf	[1,1'-Bis(diphenylphosphino)ferrocene]
EDTA	Ethylenediaminetetraacetic acid
Equiv	Equivalent
ES ⁻	Negative mode ESI
ES ⁺	Positive mode ESI
ESI	Electrospray ionization
EtOAc	Ethyl acetate
<i>J</i>	Coupling constant
M	Molar concentration
m	Multiplet
m/z	Mass to charge ratio
Me	Methyl
MeCN	Acetonitrile
MeOH	Methanol
mg	Milligram
MHz	Mega hertz
Min	Minute(s)
mL	Millilitre
mM	millimolar
mmol	Millimole
Mol	mole
MS	Low resolution mass spectrometry
NMR	Nuclear Magnetic Resonance
o	Ortho
p	para
PE	Petroleum ether bp 60-90 °C
Ph	Phenyl
ppm	Parts per million
q	Quartet
quint	Quintet
rt	Room temperature
TFA	Trifluoroacetic acid
TMS	Tetramethylsilane
µL	Microlitre

Supporting information references and notes

1. Wang, W.; Marimuthu, A.; Tsai, J.; Kumar, A.; Krupka, H. I.; Zhang, C.; Powell, B.; Suzuki, Y.; Nguyen, H.; Tabrizizad, M.; Luu, C.; West, B. L. Structural characterization of autoinhibited c-Met kinase produced by coexpression in bacteria with phosphatase. *Proc. Natl. Acad. Sci. U. S. A.* **2006**, *103*, 3563-3568.
2. D'Angelo, N. D.; Bellon, S. F.; Booker, S. K.; Cheng, Y.; Coxon, A.; Dominguez, C.; Fellows, I.; Hoffman, D.; Hungate, R.; Kaplan-Lefko, P.; Lee, M. R.; Li, C.; Liu, L.; Rainbeau, E.; Reider, P. J.; Rex, K.; Siegmund, A.; Sun, Y.; Tasker, A. S.; Xi, N.; Xu, S.; Yang, Y.; Zhang, Y.; Burgess, T. L.; Dussault, I.; Kim, T. S. Design, synthesis, and biological evaluation of potent c-Met inhibitors. *J. Med. Chem.* **2008**, *51*, 5766-5779.
3. Collie, G. W.; Koh, C. M.; O'Neill, D. J.; Stubbs, C. J.; Khurana, P.; Eddershaw, A.; Snijder, A.; Mauritzson, F.; Barlind, L.; Dale, I. L.; Shaw, J.; Phillips, C.; Hennessy, E. J.; Cheung, T.; Narvaez, A. J. Structural and Molecular Insight into Resistance Mechanisms of First Generation cMET Inhibitors. *ACS Med. Chem. Lett.* **2019**, *10*, 1322-1327.
4. Zhan, Z.; Ai, J.; Liu, Q.; Ji, Y.; Chen, T.; Xu, Y.; Geng, M.; Duan, W. Discovery of Anilinopyrimidines as Dual Inhibitors of c-Met and VEGFR-2: Synthesis, SAR, and Cellular Activity. *ACS Med. Chem. Lett.* **2014**, *5*, 673-678.
5. Soini, J.; Ukkonen, K.; Neubauer, P. High cell density media for Escherichia coli are generally designed for aerobic cultivations - consequences for large-scale bioprocesses and shake flask cultures. *Microb. Cell Fact.* **2008**, *7*, 1-11.
6. Dalvit, C.; Pevarello, P.; Tato, M.; Veronesi, M.; Vulpetti, A.; Sundstrom, M. Identification of compounds with binding affinity to proteins via magnetization transfer from bulk water. *J. Biomol. NMR* **2000**, *18*, 65-68.
7. Kabsch, W. XDS. *Acta Crystallogr. D* **2010**, *66*, 125-132.
8. Winter, G. xia2: an expert system for macromolecular crystallography data reduction. *J. Appl. Crystallogr.* **2010**, *43*, 186-190.
9. Winter, G.; Waterman, D. G.; Parkhurst, J. M.; Brewster, A. S.; Gildea, R. J.; Gerstel, M.; Fuentes-Montero, L.; Vollmar, M.; Michels-Clark, T.; Young, I. D.; Sauter, N. K.; Evans, G. DIALS: implementation and evaluation of a new integration package. *Acta Crystallogr. D* **2018**, *74*, 85-97.
10. Vonrhein, C.; Flensburg, C.; Keller, P.; Sharff, A.; Smart, O.; Paciorek, W.; Womack, T.; Bricogne, G. Data processing and analysis with the autoPROC toolbox. *Acta Crystallogr. D* **2011**, *67*, 293-302.
11. Winn, M. D.; Ballard, C. C.; Cowtan, K. D.; Dodson, E. J.; Emsley, P.; Evans, P. R.; Keegan, R. M.; Krissinel, E. B.; Leslie, A. G.; McCoy, A.; McNicholas, S. J.; Murshudov, G. N.; Pannu, N. S.; Potterton, E. A.; Powell, H. R.; Read, R. J.; Vagin, A.; Wilson, K. S. Overview of the CCP4 suite and current developments. *Acta Crystallogr. D* **2011**, *67*, 235-242.
12. Cui, J. J.; Tran-Dube, M.; Shen, H.; Nambu, M.; Kung, P. P.; Pairish, M.; Jia, L.; Meng, J.; Funk, L.; Botrous, I.; McTigue, M.; Grodsky, N.; Ryan, K.; Padrique, E.; Alton, G.; Timofeevski, S.; Yamazaki, S.; Li, Q.; Zou, H.; Christensen, J.; Mroczkowski, B.; Bender, S.; Kania, R. S.; Edwards, M. P. Structure based drug design of crizotinib (PF-02341066), a potent and selective dual inhibitor of mesenchymal-epithelial transition factor (c-MET) kinase and anaplastic lymphoma kinase (ALK). *J. Med. Chem.* **2011**, *54*, 6342-6363.
13. McCoy, A. J.; Grosse-Kunstleve, R. W.; Adams, P. D.; Winn, M. D.; Storoni, L. C.; Read, R. J. Phaser crystallographic software. *J. Appl. Crystallogr.* **2007**, *40*, 658-674.
14. Emsley, P.; Cowtan, K. Coot: model-building tools for molecular graphics. *Acta Crystallogr. D* **2004**, *60*, 2126-2132.
15. Bishop, B. C.; Cameron, M.; Cottrell, I. F.; Hands, D. Synthesis of azaindoles. GB2298199A, **1996**.
16. Hands, D.; Bishop, B.; Cameron, M.; Edwards, J. S.; Cottrell, I. F.; Wright, S. H. B. A convenient method for the preparation of 5-, 6-, and 7-azaindoles and their derivatives. *Synthesis* **1996**, 877-882.
17. Ibrahim, P. N.; Artis, D. R.; Bremer, R.; Habets, G.; Mamo, S.; Nespi, M.; Zhang, C.; Zhang, J.; Zhu, Y.-L.; Zuckerman, R.; West, B.; Suzuki, Y.; Tsai, J.; Hirth, K.-P.; Bollag, G.; Spevak, W.; Cho, H.; Gillette, S. J.; Wu, G.; Zhu, H.; Shi, S. Pyrrolo[2,3-b]pyridine derivatives as protein kinase inhibitors and their preparation, pharmaceutical compositions and use in the treatment of diseases. WO2007002433A1, **2007**.
18. Synthesised according to: Greenwood, R.; Yeung, K. The synthesis of novel pyrrololactams and their boronate ester derivatives. *Tetrahedron Letters* **2016**, *57*, 5812-5814.
19. Synthesised according to: McCoull, W.; Hennessy, E. J.; Blades, K.; Box, M. R.; Chuaqui, C.; Dowling, J. E.; Davies, C. D.; Ferguson, A. D.; Goldberg, F. W.; Howe, N. J.; Kemmitt, P. D.; Lamont, G. M.; Madden, K.; McWhirter, C.; Varnes, J. G.; Ward, R. A.; Williams, J. D.; Yang, B. Identification and optimisation of 7-azaindole PAK1 inhibitors with improved potency and kinase selectivity. *MedChemComm* **2014**, *5*, 1533-1539.